USING p-REFINEMENT TO INCREASE BOUNDARY DERIVATIVE CONVERGENCE RATES

DAVID WELLS AND JEFFREY BANKS

Abstract. Many important physical problems, such as fluid structure interaction or conjugate heat transfer, require numerical methods that compute boundary derivatives or fluxes to high accuracy. This paper proposes a novel approach to calculating accurate approximations of boundary derivatives of elliptic problems. We describe a new continuous finite element method based on p-refinement of cells adjacent to the boundary that increases the local degree of the approximation. We prove that the order of the approximation on the p-refined cells is, in 1D, determined by the rate of convergence at the mesh vertex connecting the higher and lower degree cells and that this approach can be extended, in a restricted setting, to 2D problems. The proven convergence rates are numerically verified by a series of experiments in both 1D and 2D. Finally, we demonstrate, with additional numerical experiments, that the p-refinement method works in more general geometries.

Key words. Finite elements, superconvergence, elliptic equations, numerical analysis, scientific computing.

1. Introduction

Simulation of many important physical problems, such as fluid structure interaction and conjugate heat transfer, requires numerical methods that compute boundary derivatives or fluxes to high accuracy. In some circumstances the only desired result of a calculation is a quantity derived from the boundary derivatives, such as a flux or stress: this problem has long been recognized as one of importance, and a variety of methods (see, e.g., [12, 16, 28]) have been proposed that allow reconstruction of an accurate boundary flux from less accurate interior data. Accurate boundary derivatives are also required for some numerical boundary conditions. For example, in [23] the authors presented a new discrete boundary condition for a fluid-structure interaction problem based on matching accelerations, instead of velocities, and obtained a traction boundary condition involving second derivatives of the fluid velocity. This boundary condition was the key ingredient in a new partitioned algorithm that was high-order, partitioned, and stable without subiterations. While standard in the finite difference community (see, e.g., [9, 23]) these equations, usually called *compatibility boundary conditions*, are not commonly used in finite element methods, though they have appeared in some recent work [8].

A variety of algorithms have been proposed for calculating higher order derivative values from lower order data calculated by a finite element method (see, e.g., [11, 17, 28, 29, 30]): most of these algorithms rely on *data post-processing*, where one uses least squares or other fitting procedure to fit a higher-degree polynomial through known superconvergence points, as discussed in [3]. Another class of methods relies on the application of high-order finite difference stencils to data derived on either a uniform or quasi-uniform grid [19]. A common feature of several postprocessing techniques is that they require a grid satisfying some smoothness condition: without
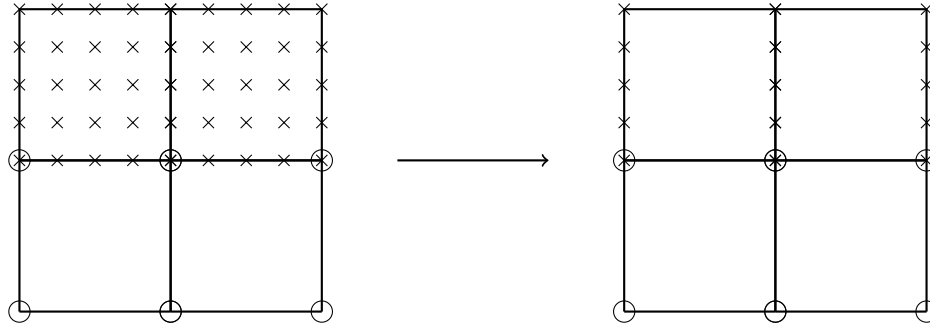
FIGURE 1. Two different implementations of p-refinement for boundary cells adjacent to interior bilinear cells, where the finite element spaces are chosen as nodal interpolants. The diagram on the left is of Q^1 elements adjacent to Q^4 elements: the degrees of freedom with support points along the two common faces would ordinarily be constrained in a way that makes the solution continuous. The scheme proposed in Section 3 uses a similar procedure to constrain *all* such nonnormal degrees of freedom on each boundary cell, effectively reducing the local approximation space to tensor products of $P^1(x)$ and $P^4(y)$. Since the degree of the approximation in the normal direction determines the derivative convergence rates, one could obtain the same effect by adding degrees of freedom corresponding to normal derivatives on the boundary instead of doing Lagrange p-refinement.

such a condition, the error in the solution may be dominated by pollution error from grid irregularities; see Chapter 4 of [3] for additional information on the impact of grid regularity. In particular, of the three most common versions of the finite element method (h-refinement based, p-refinement based, and hp-refinement based) these postprocessing methods are almost always based on estimates from the h-refinement version.

This paper proposes a novel alternative to current techniques. We present a boundary cell p-*refinement* (i.e., locally increasing the degree of the approximation space) strategy to improve the accuracy of boundary derivatives instead of postprocessing the solution. The numerical experiments in Section 4 use Lagrange p-refinement to increase the local approximation degree: a possible alternative to this is to add degrees of freedom corresponding to normal derivatives on the boundary. This p-refinement results in higher rates of convergence in the normal derivatives along the boundary. The theoretical results are based on the two-dimensional linear convection-diffusion-reaction problem

(1)
$$-\Delta u + \vec{b} \cdot \nabla u + cu = f$$

with homogeneous Dirichlet boundary conditions in y, periodic boundary conditions in x, normalized viscosity, constant advection velocity $\vec{b}$, constant reaction rate $c > 0$ (which is the standard well-posedness assumption; see Lemma 5.1 in [26] or Chapters 3 and 4 of [24] for further discussion and justification), and forcing f.
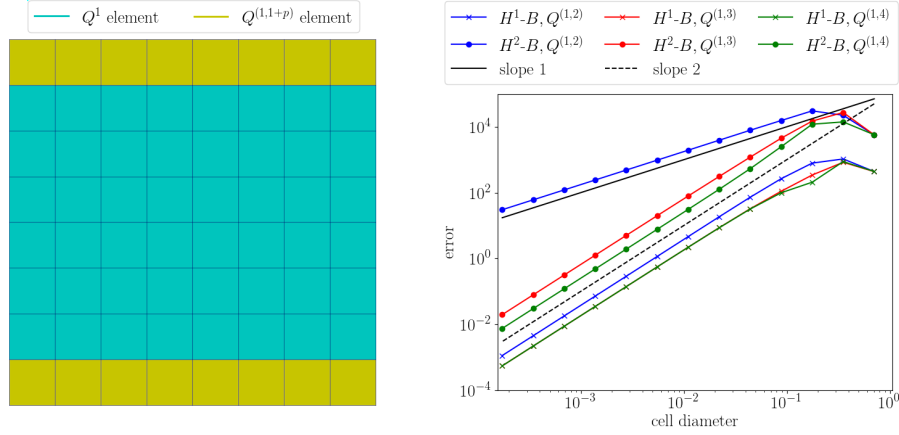
FIGURE 2. Convergence rates for a numerical approximation of (1) on a domain with periodic boundary conditions in the x direction and Dirichlet boundary conditions in the y direction. The grid on the left depicts which cells have been p-refined; the plot on the right shows convergence rates in the seminorms defined by Equations (2)-(3). The cyan cells have Q^1 (bilinear) shape functions; the yellow cells have been p-refined in the normal direction (i.e., they are $P^m \otimes P^{m+p}$ elements, notated as $Q^{(m,m+p)}$).

Our main goal is to improve the accuracy of the finite element approximation to Equation (1)'s normal derivatives along the Dirichlet boundary, notated as $\partial\Omega$. We will improve the accuracy by performing p-refinement in the direction normal to $\partial\Omega$. *p-refinement in the normal direction* means that, rather than standard Q^m elements, the polynomial space on each boundary cell is $P^m \otimes P^{m+p}$; i.e., a tensor product between degree m polynomials in the tangential direction and degree $m+p$ polynomials in the normal direction. Notate these spaces by $Q^{(m,m+p)}$, where $p \geq 0$. An example implementation of this type of p-refinement is shown on the right in Figure 1, with numerical results shown in Figure 2. The error estimates proven in this paper rely on the tensor product discretization and, as a result, provide convergence rates at mesh vertices. Hence, the numerical experiments in Section 4 show convergence rates computed in the H^1-B and H^2-B seminorms, which are defined in terms of the gradient, Hessian, and normal derivatives along the non-periodic boundary:

$$
\begin{aligned}
&|u - u^h|_{H^1\text{-}B} \\
(2) \quad &= \max_{i,j} \left| (\nabla(u - u^h) \cdot \vec{n})(\delta_i, \delta_j) : (\delta_i, \delta_j) \text{ are cell vertices on the boundary} \right|
\end{aligned}
$$

$$
\begin{aligned}
&|u - u^h|_{H^2\text{-}B} \\
(3) \quad &= \max_{i,j} \left| (\vec{n}^T \nabla^2(u - u^h)\vec{n})(\delta_i, \delta_j) : (\delta_i, \delta_j) \text{ are cell vertices on the boundary} \right|.
\end{aligned}
$$

The proposed p-refinement method does not neatly fit into the usual taxonomy of the three common versions of the finite element method. The proven convergence rates depend on the cell diameters but use multiple (fixed) polynomial orders in the domain, which resembles p-refinement: however, this is not a p-refinement method

since the refinement in p is static (i.e., only cells adjacent to the nonperiodic boundary are p-refined, and the degrees m and $m + p$ are fixed during grid refinement) and not dependent on any a-posteriori error or regularity estimator. As such, this method is not well described by the standard hp-finite element error estimate [1]

$$(4) \qquad \|u - u^{hp}\|_{H^1(\Omega)} \le Ch^{\mu}p^{-(m-1)}\|u\|_{H^m(\Omega)}$$

for elliptic problems in an energy norm, where $\mu = \min(p, m-1)$, p is the polynomial order, and the grid is quasiuniform with cell diameter h. Additionally, this method is not well-described by the classic p-refinement estimate

$$(5) \qquad \|u - u^h\|_{H^1} \le Cp^{-(m-1)}\|u\|_{H^m}$$

given in [4] since the degree p is fixed during the refinement process.

The rest of this paper is organized as follows: Section 2 presents the essential theory for a one-dimensional version of the proposed scheme, including proofs showing that performing p-refinement on boundary cells improves the boundary derivative convergence rates. Section 3 extends these results to higher dimensions: for structured grids and suitable finite elements, one can recover essentially the same convergence results from the 1D case at mesh vertices along the boundary of the domain. Finally, Section 4 summarizes some numerical experiments that demonstrate the proven asymptotic convergence rates and show that the results are still valid in a simple but non-Cartesian geometry. Section 5 concludes with a summary of the presented results and some conjectures regarding possible extensions of this work.

2. One-dimensional analysis of the model problem

2.1. Introduction. The numerical scheme for the model problem described in Section 1 may be analyzed, in part, by applying an analog of the discrete Fourier transform in the periodic direction to reduce it to a one-dimensional problem. Therefore, we begin our analysis of the discretization of Equation (1) by analyzing the simpler model

$$(6) \qquad -u_{yy} + bu_y + \tilde{c}u = \tilde{f}(y)$$

with homogeneous Dirichlet boundary conditions and, having applied a discrete Fourier transform, $\mathrm{Re}\,(\tilde{c}) > 0$ and $\tilde{c}$ and $\tilde{f}(y)$ may be complex. The primary result of this section is an analysis of the p-refinement scheme in a single space dimension for Equation (6).

It is well known (a full proof is given in [14]) that, for Equation (6), the rate of convergence of a finite element approximation u^h to the weak form of (6) consisting of continuous piecewise polynomials of order m at a mesh vertex (a point connecting two cells) y_j is

$$(7) \qquad |u^h(y_j) - u(y_j)| = O(\Delta y^{2m}),$$

where m is the degree of the polynomial space used in the two adjacent cells and all cells have diameter Δy. Subsection 2.3 presents a special case of this theorem for the last interior vertices (i.e., the interior vertices of the two boundary cells), showing that the approximation gains one additional order of accuracy at these two points. This is significantly better than the standard superconvergence result at the Gauss-Lobatto points of the function value of (see, e.g., the table in Section 1.10 of [25])

$$(8) \qquad |u^h(y_g) - u(y_g)| = O(\Delta y^{m+2}).$$

The authors of [14] note that one could perform local p-refinement and achieve higher order accuracy on a specific cell due to the higher convergence order at the mesh vertices. This is the primary idea used to achieve higher order derivative boundary convergence. The proofs of these results rely on computations with Greens' functions and, as such, do not have immediate extensions to higher dimensions due to the nonintegrability of higher-dimension Greens' functions (see the discussion regarding Greens' functions in [3] for additional information on the limitations of this approach).

2.2. Well-posedness of the system. This subsection presents some basic analysis of Equation (6). Assuming that the solution is complex-valued since the forcing and low-order coefficient may be complex, let $H_0^1([0, L])$ be the Hilbert space of complex-valued functions whose derivatives and function values are square-integrable on $[0, L]$ and have a value of zero at 0 and L. Consider the sesquilinear and skew-linear forms associated with Equation (6):

$$(9) \qquad a(\phi, \psi) = \int_0^L \phi_y \bar{\psi}_y \, dy + b \int_0^L \phi_y \bar{\psi} \, dy + \tilde{c} \int_0^L \phi \bar{\psi} \, dy$$

$$(10) \qquad l(\psi) = \int_0^L \tilde{f} \bar{\psi} \, dy.$$

The weak problem is, for a Hilbert space $X \subseteq H_0^1([0, L])$, finding $z \in X$ such that, for all $\psi \in X$

$$(11) \qquad a(z, \psi) = l(\psi).$$

Theorem 1. *The weak problem given by Equation* (11) *and a Hilbert space* $X \subseteq H_0^1([0, L])$ *is well-posed when* $\operatorname{Re}(\tilde{c}) > 0$.

Proof. This theorem immediately follows from the complex-valued version of the Lax-Milgram Theorem; see Chapter 6, Theorem 6 of [22]. Since

$$(12a) \qquad |a(\phi, \psi)| = \left| \int_0^L \phi_y \bar{\psi}_y \, dy + b \int_0^L \phi_y \bar{\psi} \, dy + \tilde{c} \int_0^L \phi \bar{\psi} \, dy \right|$$

$$(12b) \qquad \leq \gamma \|\phi\|_{H^1} \|\psi\|_{H^1}, \forall \phi, \psi \in H_0^1([0, L]),$$

the sesquilinear form is bounded with boundedness constant

$$(13) \qquad \gamma = (1 + |b| + |\tilde{c}|).$$

To show coercivity, decompose $\phi(y)$ and $\tilde{c}$ into real and imaginary components

$$(14) \qquad \phi = \phi_R + \phi_I I \text{ and } \tilde{c} = \operatorname{Re}(\tilde{c}) + \operatorname{Im}(\tilde{c}) I$$

where, to avoid confusion with the mesh vertex index i, notate $\sqrt{-1} = I$ and obtain, again $\forall \phi \in H_0^1([0, L])$,

$$(15a) \qquad |a(\phi, \phi)| \geq |\operatorname{Re}(a(\phi, \phi))|$$

$$(15b) \qquad = \left| \|\phi_y\|_{L^2}^2 + b \int_0^L (\phi_R \phi_{R,y} + \phi_I \phi_{I,y}) \, dy + \operatorname{Re}(\tilde{c}) \|\phi\|_{L^2}^2 \right|$$

$$(15c) \qquad \geq \alpha \|\phi\|_{H^1}^2$$

due to the assumption of homogeneous boundary conditions with coercivity constant

$$(16) \qquad \alpha = \min(1, \operatorname{Re}(\tilde{c})).$$

Applying the Lax-Milgram Theorem yields the stated result.   □

2.3. Superconvergence at vertices near the boundary. The primary result of this section, Theorem 2, depends on the rate of convergence of the interpolation of a smooth function on a single cell in a finite element discretization: in particular, the scaling of the derivatives of the interpolated function and the diameter of the cell play a key role in Theorem 2. Hence, this subsection begins with a special case of the Bramble-Hilbert lemma (see, e.g., [13] for a proof of the general case):

Lemma 1. *Let $K = [a, a + \Delta y]$ be an interval with diameter Δy. Let $v \in V$ where $V = W^{m+1,\infty}(K)$. Consider a finite element space $V^h \subset H^1(K), V^h = P^m(K)$, where $P^m(K)$ is the space of degree m polynomials on the interval K. Define the interpolation operator $\Pi : V \to V^h$ such that*

$$(17) \qquad (\Pi u)(\xi_j) = u(\xi_j), \Pi u \in V^h \ \text{where} \ \xi_j = a + \frac{j}{m}\Delta y, j = 0, 1, \cdots, m.$$

Then $v^h = \Pi v$ satisfies the error estimate

$$(18) \qquad\qquad \|v - v^h\|_{H^1(K)}^2 \leq \hat{C}\Delta y^{2m+1}\|v^{(m+1)}\|_{L^\infty(K)}^2$$

where $\hat{C}$ is independent of Δy and v.

Proof. This lemma follows immediately from applying Theorem 3.1.5 of [13] with parameters $m = 0$, $q = 2$, and $p = \infty$ and $m = 1$, $q = 2$, and $p = \infty$ and then summing the squares of the results.   □

Remark 1. *The same result holds for more general interpolation operators that also interpolate derivative values of the function (i.e., for Hermite-type elements), or for nonuniform point distributions (e.g., using the Gauss-Lobatto points as nodes).*

Theorem 2 is a special case for the mesh vertex located at $L - \Delta y$ (i.e., the last interior vertex) of the more general vertex convergence rate proven in [14].

Theorem 2. *Consider a partition of $[0, L]$ into N cells of equal diameter Δy. Let $V^h \subset H_0^1([0, L])$ be the finite element space of piecewise continuous polynomials of degree m on interior cells and degree $m + p$ on boundary cells, where $p \geq 1$. Define the interpolation operator $\Pi : H_0^1([0, L]) \to V^h$ on each cell in the same way as Equation (17), where interior cells have $m + 1$ interpolation points and boundary cells have $m + p + 1$ interpolation points (including, in both cases, cell vertices). Let $u^h(y) \in V^h$ be the solution to (11) with $X = V^h$. Let $u(y) \in W^{m+1,\infty}([0, L])$ be the solution of Equation (11) with $X = W^{m+1,\infty}([0, L])$. Assume that*

$$(19) \qquad\qquad D = \frac{\sqrt{b^2 + 4\tilde{c}}}{2}, \text{Re}\,(D) \geq 1, \ \text{and} \ \text{Re}\,(D) \geq |\text{Im}\,(D)|.$$

To simplify some inequalities, assume that

$$(20a) \qquad\qquad\qquad\qquad b \geq 0$$

$$(20b) \qquad\qquad\qquad\qquad L \geq 1.$$

Then there exists a constant $C_1(m, p, n, b, L) = C_1$ dependent only on m, p, n, b, and L such that

$$(21) \qquad |u(L - \Delta y) - u^h(L - \Delta y)| \leq \frac{\gamma^2}{\alpha}|D|^{m+1}\sqrt{C_1}\|u^{(m+1)}\|_{L^\infty([0,L])}\Delta y^{2m+1}$$

where γ and α are the boundedness and coercivity constants defined in Equations (13) and (16).

Proof. This proof relies on some elementary inequalities that are true due to the bounds on $|D|$ and L (for proofs, see Appendix A):

(22a)
$$\left| \frac{\exp(-2D\Delta y) - 1}{2D} \right| \leq \Delta y$$

(22b)
$$\left| \frac{\exp(2DL) \pm \exp(2D\Delta y)}{\exp(2DL) - 1} \right| \leq 4$$

(22c)
$$\left| \frac{\exp(-D(L + \Delta y - y)) \pm \exp(D(L - \Delta y - y))}{2D} \right| \leq \frac{1}{|D|}.$$

This proof follows the outline of the classic superconvergence result in [14]. Consider the Greens' function $G(y)$ associated with the operator implied by (6) and the point force δ centered at $L - \Delta y$. This Greens' function is defined by the following equations:

(23)
$$-G_{yy}(y) + bG_y(y) + \tilde{c}G(y) = \delta(y - (L - \Delta y))$$

(24)
$$G(0) = 0$$

(25)
$$[G(L - \Delta y)] = 0$$

(26)
$$[G_y(L - \Delta y)] = 1$$

(27)
$$G(L) = 0$$

i.e., $G(y)$ has homogeneous boundary conditions, is continuous at $L - \Delta y$, and has a jump in its derivative at $L - \Delta y$. This implies, by standard Greens' function calculations (see, e.g., [20]) that
(28)
$$G(y) = \begin{cases} G^L(y) = (c_1 \cosh{(Dy)} + c_2 \sinh{(Dy)}) \exp{\left(\frac{1}{2} by\right)} & 0 \leq y \leq L - \Delta y \\ G^R(y) = (c_3 \cosh{(Dy)} + c_4 \sinh{(Dy)}) \exp{\left(\frac{1}{2} by\right)} & L - \Delta y < y \leq L. \end{cases}$$

Enforcing the four conditions listed above yields

(29a)
$$c_1 = 0$$

(29b)
$$c_2 = -\frac{\cosh{(A_2)} \sinh{(DL)} - \cosh{(DL)} \sinh{(A_2)}}{A_1 D \sinh{(DL)}}$$

(29c)
$$c_3 = -\frac{\sinh{(A_2)}}{A_1 D}$$

(29d)
$$c_4 = \frac{\cosh{(DL)} \sinh{(A_2)}}{A_1 D \sinh{(DL)}}$$

where

(30a)
$$A_1 = \exp{\left(\frac{1}{2} b(L - \Delta y)\right)}$$

(30b)
$$A_2 = (L - \Delta y)D.$$

Define product decompositions $G^L(y) = G_1^L(y)G_2^L(y)$ and $G^R(y) = G_1^R(y)G_2^R(y)$, where

$$(31a) \qquad\qquad G_1^L(y) = c_2 \sinh(Dy)$$

$$(31b) \qquad\qquad G_2^L(y) = \exp\left(\frac{1}{2}by\right)$$

$$(31c) \qquad\qquad G_1^R(y) = c_3 \cosh(Dy) + c_4 \sinh(Dy)$$

$$(31d) \qquad\qquad G_2^R(y) = \exp\left(\frac{1}{2}by\right).$$

As

$$(32) \qquad\qquad \frac{d^n}{dy^n}G_1^L(y) = \begin{cases} c_2 D^n \sinh(Dy) & n \text{ is even} \\ c_2 D^n \cosh(Dy) & n \text{ is odd} \end{cases}$$

the moduli of derivatives of $G_1^L(y)$ are maximized at $y = L - \Delta y$ by the maximum modulus principle and the bound on the imaginary part given by the assumption in Equation (19). Similarly, by Assumption (20a), $G_2^L(y)$ and all of its derivatives are maximized at the same point. Putting these together, derivatives of $G_1^L(y)$ are bounded by

$(33a)$
$$\left|\frac{d^n}{dy^n}G_1^L(y)\right|_{y=L-\Delta y} = \left|D^n \frac{\exp(2DL) - (-1)^n \exp(2D\Delta y)}{\exp(2DL) - 1} \frac{\exp(-2D\Delta y) - 1}{2D}\right.$$
$$\left. \times \exp\left(\frac{1}{2}b\left(\Delta y - L\right)\right)\right|$$

$$(33b) \qquad\qquad \leq 4|D|^n \Delta y \exp\left(\frac{1}{2}b\left(\Delta y - L\right)\right)$$

$$(33c) \qquad\qquad \leq 4|D|^n \Delta y$$

by Equation (22a) and Equation (22b). Notate the bound on derivatives of $G_2^L(y)$ and $G_2^R(y)$ as

$$(34) \qquad\qquad \Gamma(b, L, n) = \Gamma = \max\left(1, \left(\frac{1}{2}b\right)^n\right) \exp\left(\frac{1}{2}bL\right).$$

Since $1 \leq |D|$, the Leibniz rule provides a max norm estimate for derivatives of $G^L(y)$:

$$\left\|\frac{d^n}{dy^n}G^L(y)\right\|_{L^\infty([0,L-\Delta y])} = \left\|\sum_{i=0}^n \binom{n}{i}\left(\frac{d^{n-i}}{dy^{n-i}}G_1^L(y)\right)\left(\frac{d^i}{dy^i}G_2^L(y)\right)\right\|_{L^\infty([0,L-\Delta y])}$$

$$(35) \qquad\qquad \leq 4(n+1)!|D|^n \Gamma \Delta y.$$

Similarly, for $G_1^R(y)$ and $L - \Delta y \leq y \leq L$

$$(36a) \quad \left|\frac{d^n}{dy^n}G_1^R(y)\right| = \left|D^n \frac{\exp(-(L + \Delta y - y)D) - (-1)^n \exp((L - \Delta y - y)D)}{2D}\right.$$
$$\left. \times \frac{\exp(2DL) - \exp(2D\Delta y)}{\exp(2DL) - 1} \exp\left(\frac{1}{2}b(\Delta y - L)\right)\right|$$

$$(36b) \qquad\qquad \leq 4|D|^{n-1}.$$

Hence, application of the Leibniz rule provides

$$\left\|\frac{d^n}{dy^n}G^R(y)\right\|_{L^\infty([L-\Delta y,L])} \leq \left\|\sum_{i=0}^n \binom{n}{i}\left(\frac{d^{n-i}}{dy^{n-i}}G_1^R(y)\right)\left(\frac{d^i}{dy^i}G_2^R(y)\right)\right\|_{L^\infty([L-\Delta y,L])}$$

$$(37) \qquad\qquad \leq 4(n+1)!|D|^{n-1}\Gamma.$$

Since G is the Greens' function

$$(38a) \qquad |u^h(L-\Delta y) - u(L-\Delta y)|^2 = |(\delta(y-(L-\Delta y)), u^h - u)|^2$$

$$(38b) \qquad\qquad\qquad\qquad = |a(G, u^h - u)|^2$$

$$(38c) \qquad\qquad\qquad\qquad = |a(G - v^h, u^h - u)|^2$$

for any $v^h \in V^h$ by Galerkin orthogonality. Let $v^h = \Pi G$ be the finite element interpolation of G. By continuity of the sesquilinear form, application of Lemma (1) to every cell and summing the result, the scalings in Equation (35) and Equation (37), and Céa's lemma (see, e.g., Theorem 2.4.1 in [13])

(39a)

$$|a(G(y) - v^h, u^h - u)|^2 \leq \gamma^2 \|u^h - u\|_{H^1}^2 \|G(y) - v^h\|_{H^1}^2$$

$$(39b) \qquad\qquad \leq \left[\left(\sum_{j=0}^{N-2}\hat{C}_m\|G^{L,(m+1)}\|_{L^\infty([j\Delta y,(j+1)\Delta y])}^2 \Delta y^{2m+1}\right)\right.$$

$$\left. + \hat{C}_{m+1}\|G^{R,(m+2)}\|_{L^\infty([L-\Delta y,L])}^2 \Delta y^{2(m+1)+1}\right]\gamma^2\|u^h - u\|_{H^1}^2$$

$$(39c) \qquad\qquad \leq \left[\max(\hat{C}_m,\hat{C}_{m+1})\left(4(m+3)!|D|^{m+1}\Gamma\right)^2\right.$$

$$\left. \times \left(\Delta y^2\left(\sum_{j=0}^{N-2}\Delta y^{2m+1}\right) + \Delta y^{2(m+1)+1}\right)\right]\gamma^2\|u^h - u\|_{H^1}^2$$

$$(39d) \qquad\qquad \leq \Delta y^{2m}\left[\max(\hat{C}_m,\hat{C}_{m+1})\left(4(m+3)!|D|^{m+1}\Gamma\right)^2\right.$$

$$\left. \times \left(\Delta y^{2m+2} + \Delta y^{2(m+1)+1}\right)\right]\frac{\gamma^4}{\alpha^2}\hat{C}_m\left\|\frac{d^{m+1}}{dy^{m+1}}u\right\|_{L^\infty([0,L])}^2$$

$$(39e) \qquad\qquad \leq \frac{\gamma^4|D|^{2m+2}C_1}{\alpha^2}\|u^{(m+1)}\|_{L^\infty([0,L])}^2\Delta y^{4m+2}$$

where

$$C_1 = 16\Gamma^2\hat{C}_m\max(\hat{C}_m,\hat{C}_{m+1})((m+3)!)^2$$

$$(40) \quad = 16\left(\max\left(1,\left(\frac{1}{2}b\right)^{m+2}\right)\hat{C}_m\exp\left(\frac{1}{2}bL\right)\right)^2\max(\hat{C}_m,\hat{C}_{m+1})((m+3)!)^2$$

is a constant depending on only on m, p, n, b, and L. Taking a square root yields the final result

$$(41) \quad |u^h(L-\Delta y) - u(L-\Delta y)| \leq \frac{\gamma^2}{\alpha}|D|^{m+1}\sqrt{C_1}\|u^{(m+1)}\|_{L^\infty([0,L])}\Delta y^{2m+1}.$$

$\square$

Remark 2. *An equivalent result also holds for the mesh vertex located at $y = \Delta y$.*

Remark 3. *Since Theorem 2 depends on global error estimates as well as estimates on the boundary cells, performing additional p-refinement on the boundary cells (i.e., $p > 1$) does not change the convergence rate. Put another way, $p = 1$ is sufficient to obtain the improved convergence rate.*

Remark 4. *This result holds for any mesh vertex that is a fixed number of cells away from a boundary, e.g., for any integer j, the vertex at $L - j\Delta y$ is a factor of Δy more accurate than a vertex in the middle of the domain as long as the cells between $L - j\Delta y$ and L are p-refined.*

2.4. Rates of convergence for boundary derivatives. This subsection presents derivations of boundary derivative convergence rates for continuous finite element approximations of the one-dimensional model problem. We begin with a brief lemma showing that optimality of function values in an L^∞ norm implies optimality (i.e., losing one power of Δy for derivative taken) in the L^∞ norm:

Lemma 2. *Let $I_1 = [0, \Delta y]$. Suppose that $p(y)$ is a degree m polynomial approximation to $u(y)$ on I_1 satisfying the max norm estimate*

$$(42) \qquad \|u(y) - p(y)\|_{L^\infty(I_1)} \leq C^* \|u(y)\|_{W^{m+1,\infty}(I_1)} \Delta y^{m+1}.$$

Then

$$(43) \quad \left\| \frac{d^n}{dy^n}\left(u(y) - p(y)\right) \right\|_{L^\infty(I_1)} \leq \left[\hat{C}(m,n)\left(C^* + \frac{1}{m!}\right) + \frac{1}{(m-n)!} \right] \|u(y)\|_{W^{m+1,\infty}(I_1)} \Delta y^{m-n+1}$$

where $\hat{C}(m,n)$ is a constant dependent only on m and n.

Proof. To simplify notation, abbreviate $L^\infty(I_1)$ and $W^{m+1,\infty}(I_1)$ as L^∞ and $W^{m+1,\infty}$ since I_1 is the only relevant interval. Let $T(y)$ be the Taylor series approximation of degree m to $u(y)$ centered at 0. Note that the derivative of the Taylor series is equal to the Taylor series of the derivative. Application of the standard Taylor series remainder formula on the derivative of $u(y) - T(y)$ yields

$$(44a) \quad \left\| \frac{d^n}{dy^n}\left(u(y) - T(y)\right) \right\|_{L^\infty} = \left\| \frac{1}{(m-n)!} \int_0^y (y-t)^{(m-n)} u^{(m+1)}(t)\,dt \right\|_{L^\infty}$$

$$(44b) \qquad\qquad \leq \frac{1}{(m-n)!} \left\| \int_0^y \Delta y^{(m-n)}\,dt \right\|_{L^\infty} \left\| u^{(m+1)}(y) \right\|_{L^\infty}$$

$$(44c) \qquad\qquad \leq \frac{1}{(m-n)!} \|u(y)\|_{W^{m+1,\infty}} \Delta y^{m-n+1}.$$

As $T(y)$ is a degree m polynomial, applying an inverse estimate yields

$$
\left\| \frac{d^n}{dy^n} \left(T(y) - p(y) \right) \right\|_{L^\infty}
$$

(45a) $\leq \hat{C}(m,n)\Delta y^{-n} \left\| T(y) - p(y) \right\|_{L^\infty}$

(45b) $= \hat{C}(m,n)\Delta y^{-n} \left\| \left(u(y) - \frac{1}{m!} \int_0^y (y-t)^m u^{(m+1)}(t)dt \right) - p(y) \right\|_{L^\infty}$

(45c) $\leq \hat{C}(m,n)\Delta y^{-n} \left(\left\| u(y) - p(y) \right\|_{L^\infty} + \left\| \frac{1}{m!} \int_0^y (y-t)^m u^{(m+1)}(t)dt \right\|_{L^\infty} \right)$

(45d) $\leq \hat{C}(m,n)\Delta y^{-n} \left(C^* \left\| u^{(m+1)}(y) \right\|_{L^\infty} \Delta y^{m+1} + \frac{1}{m!} \left\| u^{(m+1)}(y) \right\|_{L^\infty} \Delta y^{m+1} \right)$

(45e) $\leq \hat{C}(m,n) \left(C^* + \frac{1}{m!} \right) \left\| u(y) \right\|_{W^{m+1,\infty}} \Delta y^{m-n+1}$

where $\hat{C}(m,n)$ comes from an inverse estimate (see Section 4.5 of [10]) that depends on norm equivalency in finite dimensional spaces and does not depend on $u(y)$ or Δy. Applying the triangle inequality yields the stated result. $\qquad\square$

Theorem 3. *Let $V^h \subset H_0^1([0,L])$ be the space of continuous piecewise polynomials defined over N cells of uniform width Δy that partition $[0,L]$ of degree m on all interior cells and degree $m+p$ on all boundary cells. Let $u^h \in V^h$ be the solution to Equation (11) where $X = V^h$ and let u be the solution to Equation (11) with $X = W^{m+p+1,\infty}([0,L])$. Define D by Equation (19). Assume that $n \leq m+p$. Then there exists a constant C_5 dependent on m, n, p, b, and L (but independent of u, D, γ, α, and Δy) such that*

$$
\left\| \frac{d^n}{dy^n} \left(u - u^h \right) \right\|_{L^\infty(I_N)}
$$

$$
\leq C_5 \Bigg[|D|^{2m+p+3} \max\left(2, \frac{2}{|D|\Delta y} \right) \frac{\gamma^4}{\alpha^2} \| u^{(m+1)} \|_{L^\infty([0,L])} \Delta y^{2m+1}
$$

(46) $\qquad\qquad + |D|^2 \frac{\gamma^2}{\alpha} \| u(y) \|_{W^{m+p+1,\infty}(I_N)} \Delta y^{m+p-n+1} \Bigg]$

Proof. Notate the error at the last interior mesh vertex as

(47) $$ e_1 = u^h(L - \Delta y) - u(L - \Delta y). $$

Consider an auxiliary equation (still of the form of Equation (6)) defined on the interval $[L - \Delta y, L]$:

$$
-w_{yy} + bw_y + \tilde{c}w = \tilde{f}
$$

(48) $$ w(L - \Delta y) = u^h(L - \Delta y) $$

$$
w(L) = u(L).
$$

Consider the difference

(49) $$ e(y) = w(y) - u(y) $$

between the solution of Equation (48) and the solution of the original BVP restricted to $[L - \Delta y, L]$. By definition, $e(y)$ satisfies the homogeneous BVP

(50)
$$-e_{yy} + be_y + \tilde{c}e = 0$$
$$e(L - \Delta y) = e_1$$
$$e(L) = 0.$$

Since $e(y)$ solves a homogeneous second-order constant-coefficient boundary value problem it has a simple closed-form solution:

(51a)
$$e(y) = \frac{e_1 \exp\left(\frac{1}{2}b(\Delta y - L)\right)}{2} \left[\frac{\exp\left(D(L-y) + \frac{1}{2}by\right)}{\sinh(D\Delta y)} - \frac{\exp\left(D(y-L) + \frac{1}{2}by\right)}{\sinh(D\Delta y)} \right]$$

(51b)
$$= \frac{e_1 \exp\left(\frac{1}{2}b(\Delta y - L)\right)}{2} \left[A(y) - B(y)\right].$$

Hence

(52)
$$\frac{d^n}{dy^n} e(y) = \frac{e_1 \exp\left(\frac{1}{2}b(\Delta y - L)\right)}{2} \left[\left(\frac{1}{2}b - D\right)^n A(y) - \left(\frac{1}{2}b + D\right)^n B(y) \right].$$

As (see Appendix B)

(53)
$$\left| \frac{\exp(z)}{\sinh(z)} \right| \leq 2 + \frac{2}{|z|}$$

setting $z = D\Delta y$ yields

(54)
$$\left| \frac{\exp(D(y-L))}{\sinh(D\Delta y)} \right| \leq \left| \frac{\exp(D\Delta y)}{\sinh(D\Delta y)} \right| \leq 2 + \frac{2}{|D|\Delta y}.$$

Since $e(y)$ is only defined for $L - \Delta y \leq y \leq L$, $|A(y)|$ is bounded by

(55)
$$|A(y)| \leq \left(2 + \frac{2}{|D|\Delta y}\right) \exp\left(\frac{1}{2}bL\right).$$

Similarly, as $|\exp(D(y-L))| \leq |\exp(D(L-y))|$, $|B(y)| \leq |A(y)|$. Hence

(56a)
$$\left| \frac{d^n}{dy^n} e(y) \right| = \left| \frac{e_1 \exp\left(\frac{1}{2}b(\Delta y - L)\right)}{2} \left[\left(\frac{1}{2}b - D\right)^n A(y) - \left(\frac{1}{2}b + D\right)^n B(y) \right] \right|$$

(56b)
$$\leq |e_1| \exp\left(\frac{1}{2}b(\Delta y - L)\right) 2 \left(\frac{1}{2}|b| + |D|\right)^n \left(2 + \frac{2}{|D|\Delta y}\right) \exp\left(\frac{1}{2}bL\right)$$

(56c)
$$= |e_1| \exp\left(\frac{1}{2}b\Delta y\right) 2 \left(\frac{1}{2}|b| + |D|\right)^n \left(2 + \frac{2}{|D|\Delta y}\right)$$

(56d)
$$\leq |e_1| \exp\left(\frac{1}{2}|b|\right) 2^{n+2} \max\left(2, \frac{2}{|D|\Delta y}\right) |D|^n$$

since $|D| \geq \frac{1}{2}|b|$.

Let $V_1^h \subset V^h$ be the space of degree $m + p$ polynomials with support restricted to the rightmost cell (that is, the cell with extent $[L - \Delta y, L]$). Notate this cell as I_N. Let $w^h \in V_1^h$ be the finite element solution to the associated weak form of (48). Since w^h is a finite element discretization whose boundary conditions match vertex (and boundary) values of u^h, $w^h = u^h$ on the rightmost cell. Consider the

L^∞ norm of the error restricted to the rightmost cell: application of Equation (56d) and Lemma (2) yields

(57a)
$$\left\|\frac{d^n}{dy^n}(u - u^h)\right\|_{L^\infty(I_N)} = \left\|\frac{d^n}{dy^n}(u - w + w - u^h)\right\|_{L^\infty(I_N)}$$

(57b)
$$\leq \left\|\frac{d^n}{dy^n}e(y)\right\|_{L^\infty(I_N)} + \left\|\frac{d^n}{dy^n}(w - w^h)\right\|_{L^\infty(I_N)}$$

(57c)
$$\leq |e_1|\exp\left(\frac{1}{2}|b|\right)2^{n+2}\max\left(2, \frac{2}{|D|\Delta y}\right)|D|^n$$
$$+ \left[\hat{C}(m + p, n)\left(C^* + \frac{1}{(m + p)!}\right) + \frac{1}{(m + p - n)!}\right]$$
$$\times \|w(y)\|_{W^{m+p+1,\infty}(I_N)}\Delta y^{m+p-n+1}.$$

The norm of $w(y)$ may be bounded by using the definition of $e(y)$:

(58)
$$\|w(y)\|_{W^{m+p+1,\infty}(I_N)} \leq \|u(y)\|_{W^{m+p+1,\infty}(I_N)} + \|e(y)\|_{W^{m+p+1,\infty}(I_N)}$$
$$\leq \|u(y)\|_{W^{m+p+1,\infty}(I_N)}$$

(59)
$$+ (m + p + 1)|e_1|\exp\left(\frac{1}{2}|b|\right)2^{m+p+2}\max\left(2, \frac{2}{|D|\Delta y}\right)|D|^{m+p}.$$

Let
(60)
$$C_2 = \max\left(1, (m + p + 1)\left[\hat{C}(m + p, n)\left(C^* + \frac{1}{(m + p)!}\right) + \frac{1}{(m + p - n)!}\right]\right).$$

Combining terms yields

$$\left\|\frac{d^n}{dy^n}(u - u^h)\right\|_{L^\infty(I_N)} \leq \left(\left[2^{n+2}|D|^n + C_2 2^{m+p+2}|D|^{m+p}\Delta y^{m+p-n+1}\right]\exp\left(\frac{1}{2}|b|\right)\right.$$

(61a)
$$\times \max\left(2, \frac{2}{|D|\Delta y}\right)|e_1|\right)$$
$$+ C_2\|u(y)\|_{W^{m+p+1,\infty}(I_N)}\Delta y^{m+p-n+1}$$
$$\leq (1 + C_2)2^{m+p+2}|D|^{m+p}\exp\left(\frac{1}{2}|b|\right)\max\left(2, \frac{2}{|D|\Delta y}\right)|e_1|$$

(61b)
$$+ C_2\|u(y)\|_{W^{m+p+1,\infty}(I_N)}\Delta y^{m+p-n+1}$$
$$\leq 2C_2\left[2^{m+p+2}|D|^{m+p}\exp\left(\frac{1}{2}|b|\right)\max\left(2, \frac{2}{|D|\Delta y}\right)|e_1|\right.$$

(61c)
$$+ \|u(y)\|_{W^{m+p+1,\infty}(I_N)}\Delta y^{m+p-n+1}\bigg].$$

Since $n \leq m + p$. Substituting in the bound for $|e_1|$ from Theorem 2 into (61b) yields

$$
\left\| \frac{d^n}{dy^n} (u - u^h) \right\|_{L^\infty(I_N)}
$$

(62a)
$$
\leq 2C_2 \left[2^{m+p+2} |D|^{m+p} \exp\left(\frac{1}{2}|b| \right) \max\left(2, \frac{2}{|D|\Delta y} \right) \right.
$$
$$
\times \left(\frac{\gamma^2}{\alpha} |D|^{m+1} \sqrt{C_1} \|u^{(m+1)}\|_{L^\infty} \Delta y^{2m+1} \right)
$$
$$
\left. + \|u(y)\|_{W^{m+p+1,\infty}(I_N)} \Delta y^{m+p-n+1} \right]
$$
$$
= 2C_2 \left[2^{m+p+2} \sqrt{C_1} \exp\left(\frac{1}{2}|b| \right) |D|^{2m+p+1} \max\left(2, \frac{2}{|D|\Delta y} \right) \right.
$$

(62b)
$$
\left. \times \frac{\gamma^2}{\alpha} \|u^{(m+1)}\|_{L^\infty([0,L])} \Delta y^{2m+1} + \|u(y)\|_{W^{m+p+1,\infty}(I_N)} \Delta y^{m+p-n+1} \right].
$$

[27] provides the bound

(63)
$$
C^* \leq C_3(m, [0, L]) D^2 \frac{\gamma^2}{\alpha}
$$

where C_3 is dependent only on the polynomial degree m and the domain. Hence

(64a)
$$
C_2 = \max\left(1, (m+p+1) \left[\hat{C}(m+p, n) \left(C^* + \frac{1}{(m+p)!} \right) + \frac{1}{(m+p-n)!} \right] \right)
$$

(64b)
$$
\leq (1 + m + p)(1 + \hat{C}(m+p, n)) (1 + C^*)
$$

(64c)
$$
\leq (1 + m + p)(1 + \hat{C}(m+p, n)) \left(1 + C_3(m, [0, L]) D^2 \frac{\gamma^2}{\alpha} \right).
$$

Let

$$
C_4(m, p, n, b)
$$

(65)
$$
= 2((1 + m + p)(1 + \hat{C}(m+p, n))) 2^{m+p+2} \max\left(1, \sqrt{C_1} \right) \exp\left(\frac{1}{2}|b| \right).
$$

Combining Equation (62b), the definition of C_4, and the lower bound of 1 on $1/\alpha, \gamma,$ and D yields

$$\left\| \frac{d^n}{dy^n} \left(u - u^h\right) \right\|_{L^\infty(I_N)}$$

(66a)

$$\leq C_4 \Bigg[\left(1 + C_3(m, [0, L]) D^2 \frac{\gamma^2}{\alpha} \right) |D|^{2m+p+1}$$

$$\times \max \left(2, \frac{2}{|D|\Delta y} \right) \frac{\gamma^2}{\alpha} \|u^{(m+1)}\|_{L^\infty([0,L])} \Delta y^{2m+1}$$

$$+ \left(1 + C_3(m, [0, L]) D^2 \frac{\gamma^2}{\alpha} \right) \|u(y)\|_{W^{m+p+1,\infty}(I_N)} \Delta y^{m+p-n+1} \Bigg]$$

$$\leq C_4(1 + C_3(m, [0, L])) \Bigg[|D|^{2m+p+3} \frac{\gamma^4}{\alpha^2} \max \left(2, \frac{2}{|D|\Delta y} \right) \|u^{(m+1)}\|_{L^\infty([0,L])} \Delta y^{2m+1}$$

(66b)

$$+ |D|^2 \frac{\gamma^2}{\alpha} \|u(y)\|_{W^{m+p+1,\infty}(I_N)} \Delta y^{m+p-n+1} \Bigg].$$

Let

(67) $$C_5 = C_5(b, m, p, n, L) = C_4(1 + C_3(m, [0, L]))$$

so C_5 is dependent on b, L, m, p, and n but independent of u and D. Hence

$$\left\| \frac{d^n}{dy^n} \left(u - u^h\right) \right\|_{L^\infty(I_N)}$$

$$\leq C_5 \Bigg[|D|^{2m+p+3} \max \left(2, \frac{2}{|D|\Delta y} \right) \frac{\gamma^4}{\alpha^2} \|u^{(m+1)}\|_{L^\infty([0,L])} \Delta y^{2m+1}$$

(68) $$+ |D|^2 \frac{\gamma^2}{\alpha} \|u(y)\|_{W^{m+p+1,\infty}(I_N)} \Delta y^{m+p-n+1} \Bigg]$$

which is the stated result. □

Remark 5. *An equivalent result also holds for the leftmost cell, i.e., the cell with extent* $[0, \Delta y]$.

Remark 6. *If the constants* $b, \tilde{c}, D$ *are all* $O(1)$ *then the derivative error bound may be conveniently written in terms of a single scaling constant* C *that varies continuously with* b *and* $\tilde{c}$ *(and depends on* m, p, *and* n*) as*

$$\left\| \frac{d^n}{dy^n} (u - u^h) \right\|_{L^\infty(I_N)}$$

(69) $$\leq C \left(\|u^{(m+1)}(y)\|_{L^\infty([0,L])} \Delta y^{2m} + \|u(y)\|_{W^{m+p+1,\infty}(I_N)} \Delta y^{m+p-n+1} \right).$$

Remark 7. $e(y)$ *represents the contribution to the error in the last cell due to coupling the finite element approximation defined on the last cell to the rest of the computational domain. Therefore there are really two convergence regimes for this problem: one regime where the coupling error dominates and another where the local error dominates.*

3. Extensions to higher dimensions

3.1. Overview. Theorem 3 can be generalized to higher dimensions when both the finite element space and mesh have a tensor product structure. Theorem 6 does this by assuming periodic boundary conditions in x to decouple the discretization into a sum of one-dimensional problems (in y) with Dirichlet boundary conditions. We assume periodicity in this analysis, since Theorem 4 requires that the one-dimensional (in the x direction) mass and stiffness matrices have identical sets of complete and orthogonal eigenvectors. The choice of periodic boundary conditions ensures that this will be true since both matrices will be circulant. For other boundary conditions this may not be true and the consequences in 4 would need to be investigated. Unlike the one-dimensional analysis performed in Section (2), we only consider the case where $c \in \mathbb{R}$ and $c > 0$. Since part of our analysis involves complex-valued test and trial functions we consider the complex weak problem. Note that, since the discrete test functions are real-valued, we still use the standard real-valued mass and stiffness matrices in the analysis below. The 2D model problem is as follows: Let V^x be the subspace of $H^1([0,1])$ of complex-valued functions periodic over $[0,1]$. Let $V^y = H_0^1([0,L])$. Consider the sesquilinear form

$$(70) \qquad a_2(\phi, \psi) = \int_0^L \int_0^1 \nabla \phi \cdot \nabla \bar{\psi} + \vec{b} \cdot \nabla \phi \bar{\psi} + c \phi \bar{\psi} \, dx dy$$

and skew linear form

$$(71) \qquad l_2(\psi) = \int_0^L \int_0^1 f \bar{\psi} \, dx dy.$$

The weak problem is, for a Hilbert space $X \subseteq V^x \otimes V^y$, finding $z \in X$ such that, for all $\psi \in X$

$$(72) \qquad a_2(z, \psi) = l_2(\psi).$$

The decomposition used below (i.e., decomposition by using the tensor product structure) is similar to the approach used in [15]. Consider the tensor product finite element space

$$(73) \qquad W^h = V^{\Delta x} \otimes V^{\Delta y}$$

where $V^{\Delta x} \subset V^x$ is the space of periodic, piecewise linear functions defined on a uniform partition of $[0,1]$ with cell width Δx and $V^{\Delta y} \subset V^y$ is the space of piecewise polynomials defined on a uniform partition of $[0,L]$ with cell width Δy, where all boundary cells (i.e., cells adjacent to the $y = 0$ or $y = L$ boundaries) have degree $1 + p$ polynomials and all other cells have degree 1 polynomials. Note that $W^h \subset V^x \otimes V^y$. As in [15], let

$$(74) \qquad (\delta_i, \delta_j)$$

be the coordinates of cell corners (i.e., the mesh vertices in 2D).

3.2. Decoupling of the 2D Problem. This subsection presents results showing that, with periodic boundary conditions and a tensor product discretization, the discrete 2D problem is equal to a sum of uncoupled 1D problems. Part of this analysis involves using test functions that are piecewise linear interpolants of Fourier modes. For the Hilbert space $V^{\Delta x}$ defined in Equation (73), define the kth Fourier mode interpolant $F_k(x) \in V^{\Delta x}$ as

$$(75) \qquad F_k(x) = \Pi \exp(2\pi I k x)$$

where Π is the nodal piecewise linear interpolation operator onto $V^{\Delta x}$ (i.e., $F_k(x_i) = \exp(2\pi Ikx_i)$ when x_i is a mesh vertex). Note that $(F_k, F_{k'})_{L^2} = 0$ when $k \neq k'$. In addition, F_k satisfies an orthogonality property with $\exp(2\pi Ik'x)$:

Lemma 3. *Let $V^{\Delta x}$ be the Hilbert space defined by Equation (73) and $F_k(x)$ be the interpolant of $\exp(2\pi Ikx)$ defined by Equation (75). Then $F_k(x)$ is orthogonal to the Fourier mode $\exp(2\pi Ik'x)$ except when $k - k'$ is a nonzero multiple of N. Furthermore, if $k = k' + jN$ (i.e., $k - k'$ is a nonzero multiple of N) then*

$$(76) \qquad \int_0^1 F_k(x)\exp(-2\pi Ik'x)dx = \frac{\sin^2(\pi k'\Delta x)}{\pi^2 k'^2 \Delta x^2}.$$

Proof. Integration by parts yields

$$\int_0^1 F_k(x)\exp(-2\pi Ik'x)dx$$

$$(77a) \quad = \sum_{i=0}^{N-1} \frac{1}{2\pi Ik'} \int_{i\Delta x}^{(i+1)\Delta x} F_k'(x)\exp(-2\pi Ik'x)dx$$

$$(77b)$$

$$= \frac{1}{2\pi Ik'} \sum_{i=0}^{N-1} \int_{i\Delta x}^{(i+1)\Delta x} \left(\exp(2\pi Iki\Delta x)\frac{\exp(2\pi Ik\Delta x)-1}{\Delta x}\right)\exp(-2\pi Ik'x)dx$$

$$(77c) \quad = \frac{\exp(2\pi Ik\Delta x)-1}{2\pi Ik'\Delta x} \sum_{i=0}^{N-1} \int_{i\Delta x}^{(i+1)\Delta x} (\exp(2\pi Iki\Delta x))\exp(-2\pi Ik'x)dx$$

$$(77d)$$

$$= \frac{\exp(2\pi Ik\Delta x)-1}{2\pi Ik'\Delta x}\left(\frac{I(\exp(-2\pi Ik'\Delta x)-1)}{2\pi k'}\right) \sum_{i=0}^{N-1} \exp(2\pi I(k-k')i\Delta x)$$

$$(77e) \quad = \frac{(\exp(2\pi Ik\Delta x)-1)(\exp(-2\pi Ik'\Delta x)-1)}{4\pi^2 k'^2 \Delta x} \sum_{i=0}^{N-1} \exp(2\pi I(k-k')i\Delta x)$$

The summation is nonzero only if $k - k' = jN \neq 0$ for some integer j. Hence $F_k(x)$ and $\exp(2\pi Ik'x)$ are orthogonal except when $k - k'$ is a nonzero multiple of N. Finally, suppose that $k = k' + jN$. Then

$$\frac{(\exp(2\pi I(k'+jN)\Delta x)-1)(\exp(-2\pi Ik'\Delta x)-1)}{4\pi^2 k'^2 \Delta x} \sum_{i=0}^{N-1} \exp(2\pi I(jN)i\Delta x)$$

$$(78a) \quad = \frac{4\sin^2(\pi k'\Delta x)}{4\pi^2 k'^2 \Delta x}(N)$$

$$(78b) \quad = \frac{\sin^2(\pi k'\Delta x)}{\pi^2 k'^2 \Delta x^2}$$

$\square$

We now present the primary result of this section.

Theorem 4. *Let $W^h = V^{\Delta x} \otimes V^{\Delta y}$ be the tensor product finite element space defined by (73). Suppose that $u^h \in W^h$ is a solution to (72) with $X = W^h$. Then*

$$(79) \qquad u^h(x,y) = \sum_{k=-N/2-1}^{N/2} F_k(x)\hat{u}_k^h(y)$$

where the $F_k(x)$ trial functions are mutually orthogonal under both the standard one-dimensional L^2 inner product for complex functions as well as the sesquilinear form given by Equation (9), where

$$(80) \qquad (F_j, F_k)_{L^2} = \int_0^1 F_j \bar{F}_k dx = \delta_{jk} \frac{\lambda_{M,k}}{\Delta x}$$

$$(81) \qquad \vec{b} = (b_0, b_1)$$

$$(82) \qquad a(F_j, F_k) = \int_0^1 F_{j,x} \bar{F}_{k,x} + b_0 F_{j,x} \bar{F}_k + c F_j \bar{F}_k dx = \delta_{jk} \frac{\lambda_{A,k}}{\Delta x}$$

where δ_{jk} is the Kronecker delta, $a(\cdot, \cdot)$ is the sesquilinear form defined by Equation (9), λ_M and λ_A are scalars, and each $\hat{u}_k^h(y)$ satisfies the one-dimensional boundary value problem

$$(83)$$
$$\int_0^L \hat{u}_{k,y}^h \bar{\phi}_y + b_1 \hat{u}_{k,y}^h \bar{\phi} + \frac{\lambda_{A,k}}{\lambda_{M,k}} \hat{u}_k^h \bar{\phi} dy = \int_0^L \int_0^1 \frac{\Delta x}{\lambda_{M,k}} f(x,y) F_k(x) \bar{\phi} dx dy, \forall \phi(y) \in V^{\Delta y}.$$

Proof. Let A and M be the stiffness and mass matrices, respectively, coming from discretizations of $a(\cdot, \cdot)$ and $(\cdot, \cdot)_{L^2}$ with standard piecewise linear hat functions. Since $V^{\Delta x}$ consists of piecewise linear functions and the boundary conditions in the x direction are periodic, both A and M are circulant matrices and therefore share the same set of mutually orthogonal eigenvectors, which are the mesh vertex values of the Fourier interpolants $F_k(x)$ defined by Equation (75). Since the ith row of A is

$$(84) \quad A_i = \left(0, 0, \cdots, \frac{-1}{\Delta x} - \frac{b_0}{2} + \frac{c\Delta x}{6}, \frac{2}{\Delta x} + \frac{4c\Delta x}{6}, \frac{-1}{\Delta x} + \frac{b_0}{2} + \frac{c\Delta x}{6}, \cdots, 0, 0 \right)$$

and, similarly, the ith row of M is

$$(85) \qquad M_i = \left(0, \quad 0, \quad \cdots, \quad \frac{\Delta x}{6}, \quad \frac{4\Delta x}{6}, \quad \frac{\Delta x}{6}, \quad \cdots, \quad 0, \quad 0 \right)$$

The classic formula for the eigenvalues of a circulant matrices provides the kth eigenvalues of M

$$(86) \qquad \lambda_{M,k} = \frac{\Delta x (2 \cos(2\pi \Delta x k) + 4)}{6}$$

and A

$$(87) \qquad \lambda_{A,k} = \frac{2c\Delta x^2 + 3 I b_0 \Delta x \sin(2\pi \Delta x k) + (c\Delta x^2 - 6) \cos(2\pi \Delta x k) + 6}{3\Delta x}.$$

Note that $\lambda_{M,k} > 0$. Since A and M have complete sets of eigenvectors, the set $\{F_k(x)\}$ is a basis for $V^{\Delta x}$. Therefore, expressing u^h in this new basis (instead of the usual hat functions) yields

$$(88) \qquad u^h = \sum_{j,m} c_{jm} F_m(x) Y_j(y), F_m(x) \in V^{\Delta x}, Y_j(y) \in V^{\Delta y}.$$

By the same argument, consider a test function $\varphi = F_k(x) Y_l(y) \in W^h$. Plugging u^h and φ into the finite element problem given by Equation (72) with $X = W^h$

yields

$$\int_0^L \int_0^1 u_x^h \bar{\varphi}_x + b_0 u_x^h \bar{\varphi} + c u^h \bar{\varphi} dx dy + \int_0^L \int_0^1 u_y^h (\bar{\varphi}_y + b_1 \bar{\varphi}) dx dy$$

(89a) $= \int_0^L \int_0^1 f \bar{\varphi} dx dy$

$$\sum_{j,m} c_{jm} \int_0^L a(F_m, F_k) Y_j(y) \bar{Y}_l(y) + (F_m, F_k)_{L^2} Y_{j,y}(y)(\bar{Y}_{l,y}(y) + b_1 \bar{Y}_l(y)) dy$$

(89b)

$$= \int_0^L \int_0^1 f \bar{\varphi} dx dy$$

$$\sum_j c_{jk} \int_0^L \frac{\lambda_{A,k}}{\Delta x} Y_j(y) \bar{Y}_l(y) + \frac{\lambda_{M,k}}{\Delta x} Y_{j,y}(y)(\bar{Y}_{l,y}(y) + b_1 \bar{Y}_l(y)) dy$$

(89c) $= \int_0^L \int_0^1 f \bar{\varphi} dx dy$

multiplying both sides by $\Delta x / \lambda_{M,k}$ yields

(90) $$\sum_j c_{jk} \int_0^L Y_{j,y}(y)(\bar{Y}_{l,y}(y) + b_1 \bar{Y}_l(y)) + \frac{\lambda_{A,k}}{\lambda_{M,k}} Y_j(y) \bar{Y}_l(y) dy$$

$$= \int_0^L \int_0^1 \frac{\Delta x}{\lambda_{M,k}} f \bar{F}_m(x) \bar{Y}_l(y) dx dy.$$

Hence, defining

(91) $$\hat{u}_k^h(y) = \sum_j c_{jk} Y_j(y)$$

yields the one-dimensional convection-diffusion-reaction problem

(92) $$\int_0^L \hat{u}_{k,y}^h(y) \bar{Y}_{l,y}(y) + b_1 \hat{u}_{k,y}^h(y) \bar{Y}_l(y) + \frac{\lambda_{A,k}}{\lambda_{M,k}} \hat{u}_k^h(y) \bar{Y}_l(y) dy = \int_0^L \hat{f}_k^h(y) \bar{Y}_l(y) dy$$

for all $Y_l(y) \in V^{\Delta y}$, where

(93) $$\hat{f}_k^h(y) = \int_0^1 \frac{\Delta x}{\lambda_{M,k}} f(x, y) \bar{F}_k(x) dx$$

is the L^2 projection of the x-component of f onto $F_k(x)$. Therefore, by construction

(94) $$u^h(x, y) = \sum_k F_k(x) \hat{u}_k^h(y)$$

where each $\hat{u}_k^h(y)$ satisfies Equation (92). □

Theorem 5. *The resulting one-dimensional finite element problem implied by Equation (92) is well-posed.*

Proof. The eigenvalue ratio is

(95) $$\lambda_k = \frac{\lambda_{A,k}}{\lambda_{M,k}} = \frac{2c\Delta x^2 + 3Ib_0 \Delta x \sin(2\pi \Delta x k) + (c\Delta x^2 - 6) \cos(2\pi \Delta x k) + 6}{\Delta x^2 (\cos(2\pi \Delta x k) + 2)}.$$

Notate the real part of the eigenvalue ratio as

$$(96) \qquad \operatorname{Re}(\lambda_k) = \frac{2c\Delta x^2 + (c\Delta x^2 - 6)\cos(2\pi\Delta xk) + 6}{\Delta x^2(\cos(2\pi\Delta xk) + 2)}.$$

Note that

$$(97a) \qquad \operatorname{Re}(\lambda_k) \geq \frac{2c\Delta x^2 + (c\Delta x^2 - 6)\cos(2\pi\Delta xk) + 6}{3\Delta x^2}$$

$$(97b) \qquad = \frac{(2 + \cos(2\pi\Delta xk))c\Delta x^2 + 6(1 - \cos(2\pi\Delta xk))}{3\Delta x^2}$$

$$(97c) \qquad \geq c$$

and

$$(98a) \qquad \operatorname{Re}(\lambda_k) \leq \frac{2c\Delta x^2 + (c\Delta x^2 - 6)\cos(2\pi\Delta xk) + 6}{\Delta x^2}$$

$$(98b) \qquad = \frac{(2 + \cos(2\pi\Delta xk))c\Delta x^2 + 6(1 - \cos(2\pi\Delta xk))}{\Delta x^2}$$

$$(98c) \qquad \leq \frac{6 + 3c\Delta x^2}{\Delta x^2}.$$

Hence, for any $\Delta x > 0$ $c < \operatorname{Re}(\lambda_k) < \infty$, so by Theorem 1 the resulting one-dimensional problem is well-posed. $\qquad\square$

Remark 8. *An unusual feature of this well-posedness argument is the presence of the continuity constant that scales like $O(1/\Delta x^2)$: this is due to the presence of two x-derivatives in the low order term of the y discretization.*

3.3. Boundary derivative convergence of the 2D problem.

Theorem 6. *Consider the discretization of Equation (1) described in Equations (70)-(73). Let C_6 and C_8 be constants dependent on the coefficients of (1), the domain, the forcing function (in particular, its regularity), and the number of derivatives n. Assume that f is at least $18 + p$ times differentiable in the y direction. This discretization recovers the 1D estimate given by Theorem 3 at isolated points along the nonperiodic boundary with an additional error term coming from the x-discretization:*

$$(99) \qquad \left| \frac{d^n}{dy^n}\left(u(x,y) - u^h(x,y)\right)\Big|_{(\delta_i,\delta_{N^*})} \right| \leq C_6\Delta x^2 + C_8(\Delta y^2 + \Delta y^{2+p-n})$$

where $N^* = 0$ or $N^* = N$.

Proof. Since $u(x,y)$ and $f(x,y)$ are periodic in the x direction and smooth they are equal to their Fourier series:

$$(100) \qquad u(x,y) = \sum_{k=-\infty}^{\infty} \exp(2\pi Ikx)\hat{u}_k(y)$$

$$(101) \qquad f(x,y) = \sum_{k=-\infty}^{\infty} \exp(2\pi Ikx)\hat{f}_k(y).$$

Hence each $\hat{u}_k$ solves the BVP

$$(102) \qquad -\hat{u}_{k,yy} + b_1\hat{u}_{k,y} + (4\pi^2k^2 + 2\pi Ib_0k + c)\hat{u}_k = \hat{f}_k$$

corresponding to the weak problem

$$(103) \qquad \int_0^L \hat{u}_{k,y}\bar{\phi}_y + b_1\hat{u}_{k,y}\bar{\phi} + (4\pi^2 k^2 + 2\pi I b_0 k + c)\hat{u}_k\bar{\phi}dy = \int_0^L \hat{f}_k\bar{\phi}dy.$$

By Equation (79), u^h may be written as

$$(104) \qquad u^h(x,y) = \sum_{k=-\infty}^{\infty} F_k(x)\hat{u}_k^h(y)$$

where, for $|k| > 1/(2\Delta x)$, $F_k(x) = \hat{u}_k^h(y) = 0$. Hence, assume that $|k| \le 1/(2\Delta x)$. The difference between the eigenvalue ratio and the low order coefficient in Equation (103) is equal to, by a Taylor series expansion in Δx,

(105a)
$$\frac{\lambda_{A,k}}{\lambda_{M,k}} = 4\pi^2 k^2 + 2I\pi b_0 k + c + \frac{4}{3}\pi^4 k^4 \Delta x^2 + \frac{1}{45}\left(8\pi^6 k^6 - 8I\pi^5 b_0 k^5\right)\Delta x^4 + \cdots$$

$$(105b) \quad = 4\pi^2 k^2 + 2I\pi b_0 k + c + R.$$

Since $|k| \le 1/(2\Delta x)$, converting all terms in the Taylor series of R to constant multiples of $k^4\Delta x^2$ or $k^4\Delta x^3$ yields

$$(106) \qquad |R| \le C_R(b_0)k^4\Delta x^2$$

where $C_R(b_0)$ is a constant dependent on b_0. Let $\hat{v}_k(y) \in V^y$ be the solution to the semidiscretization in x of Equation (70), i.e., the solution to the weak problem
(107)
$$\int_0^L \hat{v}_{k,y}\bar{\phi}_y + b_1\hat{v}_{k,y}\bar{\phi} + (4\pi^2 k^2 + 2\pi I b_0 k + c + R)\hat{v}_k\bar{\phi}dy = \int_0^L \hat{f}_k^h(y)\bar{\phi}dy, \forall \phi \in V^y$$

where $\hat{v}_k(y) = 0$ for $|k| > 1/(2\Delta x)$. The rest of the proof follows from a triangle inequality argument involving $\hat{u}_k$, $\hat{v}_k$, and $\hat{u}_k^h$. Consider the decomposition

$$u(\delta_i, y) - u^h(\delta_i, y)$$

$$(108a) \quad = \sum_{k=-\infty}^{\infty}\left(\exp(2\pi Ik\delta_i)\hat{u}_k(y) - F_k(\delta_i)\hat{u}_k^h(y)\right)$$

$$(108b) \quad = \sum_{k=-\infty}^{\infty}\left(\exp(2\pi Ik\delta_i)\hat{u}_k(y) - F_k(\delta_i)\hat{v}_k(y) + F_k(\delta_i)\hat{v}_k(y) - F_k(\delta_i)\hat{u}_k^h(y)\right)$$

$$= \sum_{k=-\infty}^{\infty}\bigg(\exp(2\pi Ik\delta_i)\left(\hat{u}_k(y) - \hat{v}_k(y)\right) + (\exp(2\pi Ik\delta_i) - F_k(\delta_i))\hat{v}_k(y)$$

$$(108c) \qquad\qquad + F_k(\delta_i)\left(\hat{v}_k(y) - \hat{u}_k^h(y)\right)\bigg)$$

$$(108d) \quad = \sum_{k=-\infty}^{\infty}\Bigg(\underbrace{\exp(2\pi Ik\delta_i)\left(\hat{u}_k(y) - \hat{v}_k(y)\right)}_{=(1)} + \underbrace{F_k(\delta_i)\left(\hat{v}_k(y) - \hat{u}_k^h(y)\right)}_{=(2)}\Bigg)$$

since $\exp(2\pi Ik\delta_i) = F_k(\delta_i)$ by the definition of $F_k(x)$ in Equation (75).

Bounding (1). Let $\hat{e}_k = \hat{v}_k - \hat{u}_k$. Then $\hat{e}_k$ satisfies the weak boundary value problem
(109)
$$\int_0^L \hat{e}_{k,y}\bar{\phi}_y + b_1\hat{e}_{k,y}\phi + (4\pi^2 k^2 + 2\pi I b_0 k + c)\hat{e}_k\bar{\phi}dy = \int_0^L \left(\left(\hat{f}_k^h - \hat{f}_k\right) - R\hat{v}_k\right)\bar{\phi}dy.$$

$\hat{e}_k$ can be bounded by standard Sobolev estimates since the right-hand side (a combination of the error in the approximate Fourier mode and error in the low order term) is relatively small ($O(\Delta x^2)$ for small k). Since $\hat{e}_k$ solves an elliptic problem with smooth data, a regularity estimate yields (see [18], section 6.3.2)
(110)
$$\|\hat{e}_k\|_{H^{r+2}} \leq C([0,L],r)\left(1 + |b_1| + \left|4\pi^2 k^2 + 2\pi I b_0 k + c\right|\right)\left\|\left(\left(\hat{f}_k^h - \hat{f}_k\right) - R\hat{v}_k\right)\right\|_{H^r}.$$

Due to the homogeneous boundary conditions, the fundamental theorem of calculus implies that

(111)
$$\left\|\frac{d^n}{dy^n}\hat{e}_k\right\|_{L^\infty} \leq L\left\|\frac{d^n}{dy^n}\hat{e}_k\right\|_{H^1} \leq L\|\hat{e}_k\|_{H^{n+1}}.$$

Combining Equations (110)-(111) yields, for $1 \leq n$,

(112a)
$$\left\|\frac{d^n}{dy^n}\hat{e}_k\right\|_{L^\infty} \leq C([0,L],n-1)\left(1 + |b_1| + \left|4\pi^2 k^2 + 2\pi I b_0 k + c\right|\right)$$
$$\times \left\|\left(\hat{f}_k^h - \hat{f}_k\right) - R\hat{v}_k\right\|_{H^{n-1}}$$

(112b)
$$\leq C([0,L],n-1)\left(1 + |b_1| + \left|4\pi^2 k^2 + 2\pi I b_0 k + c\right|\right)$$
$$\times \left(\left\|\hat{f}_k^h - \hat{f}_k\right\|_{H^{n-1}} + R\|\hat{v}_k\|_{H^{n-1}}\right).$$

Lemma 3 bounds the error in approximating $\hat{f}_k$:

(113a)
$$\hat{f}_k^h(y) - \hat{f}_k(y) = \int_0^1 \frac{\Delta x}{\lambda_{M,k}}f(x,y)\bar{F}_k(x)dx - \hat{f}_k(y)$$

(113b)
$$= \int_0^1 \frac{\Delta x}{\lambda_{M,k}}\left(\sum_{j=-\infty}^\infty \hat{f}_{k+jN}(y)\exp(2\pi I(k+jN)x)\right)\bar{F}_k(x)dx - \hat{f}_k(y)$$

$$= \left(\int_0^1 \frac{\Delta x}{\lambda_{M,k}}\exp(2\pi Ikx)\bar{F}_k(x) - 1dx\right)\hat{f}_k(y)$$

(113c)
$$+ \frac{\Delta x}{\lambda_{M,k}}\sum_{\substack{j=-\infty\\j\neq 0}}^\infty \hat{f}_{k+jN}(y)\int_0^1 \exp(2\pi I(k+jN)x)\bar{F}_k(x)dx$$

$$= \left(\frac{\sin^2(\pi\Delta xk)}{\pi^2\Delta x^2 k^2}\frac{\Delta x}{\lambda_{M,k}} - 1\right)\hat{f}_k(y)$$

(113d)
$$+ \frac{\Delta x}{\lambda_{M,k}}\sum_{\substack{j=-\infty\\j\neq 0}}^\infty \hat{f}_{k+jN}(y)\frac{4N^2\sin^2(\pi(k+jN)/N)}{\pi^2(k+jN)^2}.$$

Due to the regularity assumption on f, there exists a constant $C(f)$ independent of x, y, and k such that

$$\text{(114)} \qquad \left| \frac{d^n}{dy^n} \hat{f}_k(y) \right| \le C(f) k^{-q+n}$$

$$\text{(115)} \qquad \left| \frac{d^n}{dy^n} \hat{f}_k^h(y) \right| \le C(f) k^{-q+n}.$$

Note that

$$\text{(116)} \qquad \frac{\Delta x}{\lambda_{M,k}} = \frac{6}{2\cos(2\pi k \Delta x) + 4} \Rightarrow \left| \frac{\Delta x}{\lambda_{M,k}} \right| \le 3.$$

Substituting Equations (114) and (116) into the nth derivative of Equation (113d) yields

$$\left| \frac{d^n}{dy^n} \left(\hat{f}_k^h(y) - \hat{f}_k(y) \right) \right|$$

$$\text{(117a)} \quad \le C(f) \left(\left| \frac{\sin^2(\pi \Delta x k)}{\pi^2 \Delta x^2 k^2} \frac{\Delta x}{\lambda_{M,k}} - 1 \right| k^{-q+n} + \frac{12 N^2}{\pi^2} \sum_{\substack{j=-\infty \\ j \ne 0}}^{\infty} \frac{1}{(Nj+k)^{2+q-n}} \right)$$

$$\text{(117b)} \quad \le C(f) \left(\left| \frac{\sin^2(\pi \Delta x k)}{\pi^2 \Delta x^2 k^2} \frac{\Delta x}{\lambda_{M,k}} - 1 \right| k^{-q+n} + \frac{12 N^2}{\pi^2} \sum_{\substack{j=-\infty \\ j \ne 0}}^{\infty} \frac{1}{(Nj+k)^{2+q-n}} \right)$$

$$= C(f) \left(\left| \frac{\sin^2(\pi \Delta x k)}{\pi^2 \Delta x^2 k^2} \frac{\Delta x}{\lambda_{M,k}} - 1 \right| k^{-q+n} + \frac{12 N^2}{\pi^2} \left(N^{-2-q+n} \right) \right.$$

$$\text{(117c)} \qquad \left. \left[\zeta_H(2+q-n, 1+kN^{-1}) + \zeta_H(2+q-n, 1-kN^{-1}) \right] \right)$$

where ζ_H is the Hurwitz zeta function. Rearranging the first term in Equation (117c) and performing a Taylor series expansion of the first term around $k\Delta x = 0$ provides the bound

$$\left| \frac{\sin^2(\pi \Delta x k)}{\pi^2 k^2 \Delta x^2} \frac{6}{2\cos(2\pi k \Delta x) + 4} - 1 \right|$$

$$\text{(118a)} \qquad = \left| \frac{6}{2\cos(2\pi k \Delta x) + 4} \right| \left| \frac{\sin^2(\pi \Delta x k)}{\pi^2 k^2 \Delta x^2} - \frac{2\cos(2\pi k \Delta x) + 4}{6} \right|$$

$$\text{(118b)} \qquad \le 3 \left| \frac{\sin^2(\pi \Delta x k)}{\pi^2 k^2 \Delta x^2} - \frac{2\cos(2\pi k \Delta x) + 4}{6} \right|$$

$$\text{(118c)} \qquad = 3 \left| \sin^2(\pi \Delta x k) - \frac{2\cos(2\pi k \Delta x) + 4}{6} \pi^2 k^2 \Delta x^2 \right| \frac{1}{\pi^2 k^2 \Delta x^2}$$

$$\text{(118d)} \qquad \le 3 \left| \frac{1}{3}(k\pi\Delta x)^4 + \left(\frac{928}{3} \pi^8 (k\Delta x)^2 + 192\pi^6 \right) (k\Delta x)^6 \right| \frac{1}{\pi^2 k^2 \Delta x^2}$$

$$\text{(118e)} \qquad = 3 \left| \frac{1}{3}(k\pi\Delta x)^2 + \left(\frac{928}{3} \pi^8 (k\Delta x)^2 + 192\pi^6 \right) (k\Delta x)^4 \right|$$

$$\text{(118f)} \qquad \le C_T k^2 \Delta x^2$$

since $|k| \leq 1/(2\Delta x)$, where C_T is a constant dependent on the coefficients of the Taylor series expansion. Since

$$\text{(119)} \qquad \frac{1}{2} \leq 1 - kN^{-1}$$

The ζ_H terms are bounded by

$$\text{(120a)} \qquad \zeta_H\left(2 + q - n, \frac{1}{2}\right) = \sum_{j=0}^{\infty} \frac{1}{(\frac{1}{2} + j)^{2+q-n}}$$

$$\text{(120b)} \qquad \leq 2^{2+q-n} + \sum_{j=1}^{\infty} \frac{1}{j^2}$$

$$\text{(120c)} \qquad = 2^{2+q-n} + 1$$

due to the assumption on the regularity of f. Hence

$$\text{(121)} \qquad \zeta_H(2 + q - n, 1 + kN^{-1}) + \zeta_H(2 + q - n, 1 - kN^{-1}) \leq 2^{3+q-n} + 2.$$

Hence, substituting $N = 1/\Delta x$, Equation (118f), and Equation (121) into Equation (117c) yields

$$\left| \frac{d^n}{dy^n} \left(\hat{f}_k^h(y) - \hat{f}_k(y) \right) \right| \leq C(f) \left[\left(C_T k^2 \Delta x^2 \right) k^{-q+n} + (2^{3+q-n} + 2)\Delta x^{q-n} \right]$$

$$\text{(122)} \qquad \leq C(f) \left[C_T k^{-q+n+2} \Delta x^2 + (2^{3+q-n} + 2)\Delta x^{q-n} \right].$$

Since $\hat{v}_k$ is a weak solution to Equation (107), it satisfies the derivative estimate

$$\text{(123a)} \qquad \|\hat{v}_k\|_{H^{r+2}} \leq C([0, L], r) \left(1 + |b_1| + \left| \frac{\lambda_{A,k}}{\lambda_{M,k}} \right| \right) \|\hat{f}_k^h\|_{H^r}$$

$$\text{(123b)} \qquad \leq C([0, L], r) \left(1 + |b_1| + \left| \frac{\lambda_{A,k}}{\lambda_{M,k}} \right| \right) C(f) k^{-q+r}.$$

Hence, substituting Equation (106), Equation (122), and Equation (123b) into Equation (112b) yields

$$\left\| \frac{d^n}{dy^n} \hat{e}_k \right\|_{L^\infty} \leq C([0, L], n - 1)C(f) \left(1 + |b_1| + \left| 4\pi^2 k^2 + 2\pi I k b_0 + c \right| \right)$$

$$\times \left(C_T k^{2-q+n} \Delta x^2 + (2^{3+q-n} + 2)\Delta x^{q-n} + C_R(b_0)C([0, L], n)k^4 \Delta x^2 \right.$$

$$\text{(124a)} \qquad \times \left. \left(1 + |b_1| + \left| \frac{\lambda_{A,k}}{\lambda_{M,k}} \right| \right) k^{-q+\max(n-3,0)} \right)$$

$$\text{(124b)} \qquad \leq C_6 \left(k^{4-q+n} \Delta x^2 + (2^{3+q-n} + 2)k^2 \Delta x^{q-n} + k^{8-q+\max(n-3,0)} \Delta x^2 \right)$$

where

$$\text{(125)} \qquad C_6 = C_6([0, L], \vec{b}, c, n, C(f), C_R(b_0), C_T)$$

is a constant independent of k and Δx. Due to the regularity assumption on f the exponent is bounded by $10 + \max(n - 3, 0) \leq q$: hence this sum converges and

$$\text{(126)} \qquad \left| \sum_{k=-\infty}^{\infty} \exp(2\pi I k \delta_i) \frac{d^n}{dy^n} \hat{e}_k(y) \right| \leq C_6([0, L], \vec{b}, c, n, C(f), C_R(b_0), C_T)\Delta x^2$$

since, for $|k| > 1/(2\Delta x)$, due to the regularity assumption on f

$$(127) \qquad \left| \frac{d^n}{dy^n} \hat{e}_k(y) \right| = \left| \frac{d^n}{dy^n} \hat{u}_k(y) \right| \leq Ck^{-18+p} \leq Ck^{-16+p}\Delta x^2$$

for some constant C dependent on $C(f)$, so the contribution from the unresolved modes is also bounded by a constant multiple of Δx^2.

Bounding (2). Consider the error in the full discretization relative to the semidiscretization (i.e., $\hat{u}_k^h - \hat{v}_k$). The finite element solution $\hat{u}_k^h$ satisfies the boundary value problem

$$(128) \qquad \int_0^L \hat{u}_{k,y}^h \bar{\phi}_y + b_1 \hat{u}_{k,y}^h \bar{\phi} + \frac{\lambda_{A,k}}{\lambda_{M,k}} \hat{u}_k^h \bar{\phi} dy = \int_0^L \hat{f}_k^h \bar{\phi} dy, \ \forall \phi \in V^{\Delta y}([0,L]).$$

while the semidiscretization $\hat{v}_k$ satisfies Equation (107). Hence Theorem 3 bounds the difference between each $\hat{u}_k^h - \hat{v}_k$ term, where

$$(129) \qquad D = \frac{\sqrt{b_1^2 + \dfrac{4\lambda_{A,k}}{\lambda_{M,k}}}}{2}$$

has a positive real part since $c > 0$. Since the eigenvalue ratio is bounded by Equations (97c)-(98c), there exists a constant κ independent of k, but dependent on b_1 and c, such that

$$(130a) \qquad 1 \leq |D| \leq \kappa(1 + |k|)$$

$$(130b) \qquad \frac{\gamma}{\sqrt{\alpha}} \leq \kappa(1 + k^2)$$

due to Equation (98c) and the bound $|k| \leq 1/(2\Delta x)$. Let

$$(131) \qquad C_7 = C_7(b_1, p, n, L) = C_5(b_1, 1, p, n, L)$$

be the constant used in Theorem 3 with $m = 1$. Then, applying Theorem 3, the error in the derivative in the boundary cell I_N is

$$
\begin{aligned}
\left\| \frac{d^n}{dy^n}(\hat{v}_k - \hat{u}_k^h) \right\|_{L^\infty(I_N)} \leq & C_7 \left[|D|^{p+5} \max\left(2, \frac{2}{|D|\Delta y}\right) \frac{\gamma^4}{\alpha^2} \|\hat{v}_k^{(2)}\|_{L^\infty} \Delta y^3 \right. \\
& \left. + |D|^2 \frac{\gamma^2}{\alpha} \|\hat{v}_k\|_{W^{2+p,\infty}} \Delta y^{2+p-n} \right] \\
\leq & C_7 \left[\kappa^{p+9}(1+|k|)^{p+5}(1+k^2)^4 \max\left(2, \frac{2}{\Delta y}\right) \|\hat{v}_k^{(2)}\|_{L^\infty} \Delta y^3 \right. \\
(132) \qquad & \left. + \kappa^4(1+|k|)^2(1+k^2)^2 \|\hat{v}_k\|_{W^{2+p,\infty}} \Delta y^{2+p-n} \right]
\end{aligned}
$$

By the fundamental theorem of calculus

$$(133) \qquad \left\| \hat{v}_k^{(r)} \right\|_{L^\infty} \leq C([0,L]) \left\| \hat{v}_k^{(r)} \right\|_{H^1} \leq C([0,L]) \|\hat{v}_k\|_{H^{r+1}}$$

where $C([0,L])$ is a constant dependent on the domain. Hence, by Equation (123b)

$$(134) \qquad \|\hat{v}_k\|_{W^{2+p,\infty}} \leq C([0,L], 2+p) \left(1 + |b_1| + \left| \frac{\lambda_{A,k}}{\lambda_{M,k}} \right| \right) C(f)k^{-q+p+1}$$

where $C([0, L], 2 + p)$ is a constant dependent on both the domain and the polynomial degree. Combining the elliptic regularity estimate given by Equation (133) and the error bound given by (132) yields

$$\left\| \frac{d^n}{dy^n}(\hat{v}_k - \hat{u}_k) \right\|_{L^\infty(I_N)} \le C_7 C([0, L], 2 + p) \left(1 + |b_1| + \left| \frac{\lambda_{A,k}}{\lambda_{M,k}} \right| \right) C(f)$$

$$\times \left[\kappa^{p+9}(1 + |k|)^{p+5}(1 + k^2)^4 \max\left(2, \frac{2}{\Delta y} \right) k^{-q+1}\Delta y^3 \right.$$

$$\left. (135) \qquad + \kappa^4(1 + |k|)^2(1 + k^2)^2 k^{-q+p+1}\Delta y^{2+p-n} \right].$$

Note that the eigenvalue ratio $\lambda_{A,k}/\lambda_{M,k}$ scales like $O(k^2)$. Hence, by the assumption that $q \ge 18 + p$ the summation over k converges:

$$\sum_{k=-\infty}^{\infty} \left| \frac{d^n}{dy^n} \left(\hat{v}_k(y) - \hat{u}_k^h(y) \right) \exp(2\pi I k \delta_i) \right|$$

$$(136) \qquad = C_8([0, L], f, C_7, \vec{b}, c, p, n)(\Delta y^2 + \Delta y^{2+p-n}).$$

for a constant C_8 independent of Δx and Δy. Hence, by the triangle inequality

$$\left| \frac{d^n}{dy^n}(u - u^h) \right|_{(\delta_i, \delta_{N*})} \le C_6([0, L], \vec{b}, c, n, C(f), C_R(b_0), C_T)\Delta x^2$$

$$(137) \qquad + C_8([0, L], f, C_7, \vec{b}, c, p, n) \left(\Delta y^2 + \Delta y^{2+p-n} \right)$$

which is the desired result. □

4. Numerical Results

4.1. Overview. This section summarizes numerical experiments verifying the rates of convergence proven in Theorems 3 and 6. All experiments were performed with a finite element discretization of (1) in either one or two spatial dimensions, utilizing the `deal.II` library's [2] support for tensor product hp-finite elements. For further information on algorithms and data structures for general hp codes for continuous finite elements see [7]. The resulting linear systems were solved with the standard PETSc [5, 6] GMRES linear solver and the `BoomerAMG` algebraic multigrid preconditioner from the HYPRE library [21]. The preconditioner was configured to use SOR/Jacobi relaxation and Gaussian elimination for the coarse solve. The linear solver used a tolerance of 10^{-14} times the Euclidean norm of the right-hand side vector. We verify the rates of convergence with respect to the seminorms defined by Equations (2)-(3) from Theorem 3 and Theorem 6 by performing uniform grid refinement studies.

4.2. 1D Numerical Results. This subsection presents numerical verification of the convergence rates proven in Theorem 3 for the seminorms defined by Equations (2)-(3). We use the method of manufactured solutions to derive a forcing function for the exact solution

$$(138) \qquad u(x) = \sin(10x)$$

to Equation (6) with $b = 1$ and $c = 2$. Figures 3-4 depict the errors in the pointwise boundary first and second derivative seminorms. The resulting finite element space is notated as Q^m-Q^{m+p}, where $m \in \{1, 2\}$ is the polynomial degree on interior cells and $m + p$ (with $p \in \{0, 1, 2, 3\}$) is the polynomial degree on boundary cells. These
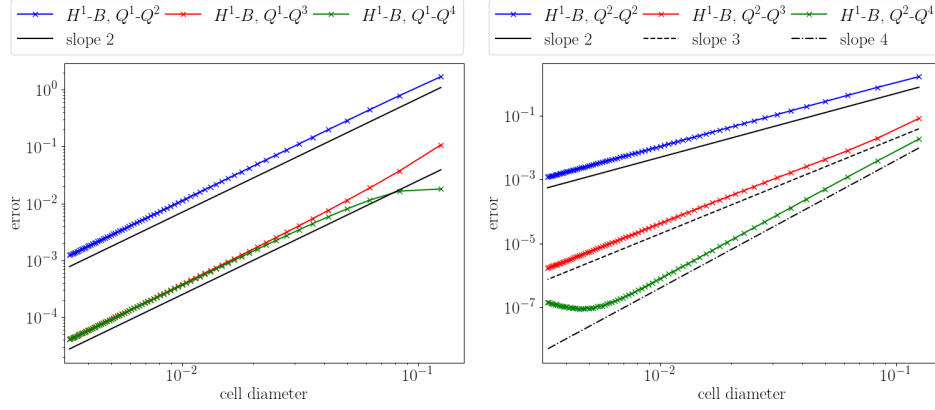
FIGURE 3.   Rates of convergence in the H^1-B seminorm with exact solution (138). The solution to the discretization using quadratic elements on the interior encounters roundoff error after sufficient grid refinement. These results verify the convergence rate proven in Theorem 3, i.e., the rate of convergence in the boundary derivatives is limited by the rate of convergence at the last interior mesh vertex and the polynomial degree on the boundary cell.
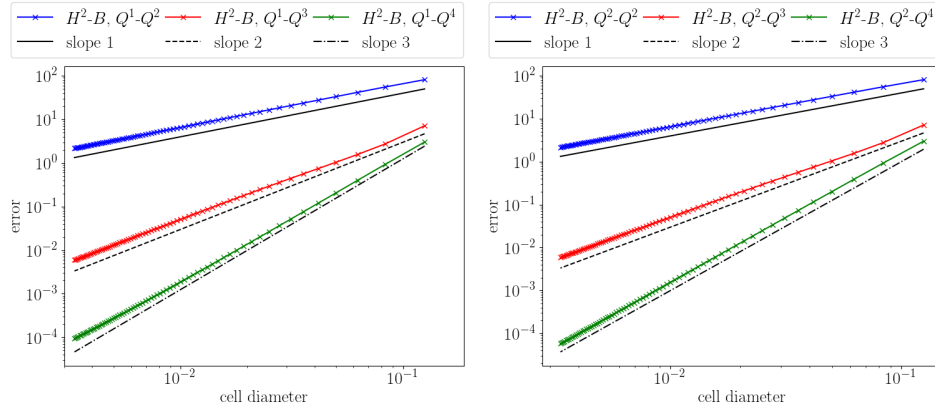

FIGURE 4. Rates of convergence in the H^2-B seminorm with exact solution (138). The second boundary derivative error with the Q^1-Q^2, Q^1-Q^3, and Q^1-Q^4 discretizations is dominated by the local error instead of the coupling error, resulting in third order convergence for sufficient boundary p-refinement.

figures illustrate the two different rates of convergence for the boundary derivatives: The error in the boundary derivative depends both on the local polynomial degree (i.e., $m+p$) and on the approximation order at the last interior mesh vertex, which is (by Theorem 2) $2m+1$. Hence, by Theorem 3 the asymptotic convergence rate for the nth derivative should be $\min(2m, m+p-n+1)$, which is what we observe in Figures 3-4.

4.3. 2D Numerical Results. This subsection presents numerical verification of the convergence rates proven in Theorem 6 (i.e., derivative convergence rates for interior bilinear elements and a periodic boundary condition along the non-enriched boundaries). Additional numerical experiments demonstrate that these improved convergence rates can be obtained in other geometries, such as a square with only Dirichlet boundary conditions and a disk. In all cases, the discretization consists of bilinear elements on all interior cells and p-refinement limited to boundary cells. All numerical experiments, unless otherwise noted, use anisotropic (i.e., only in the normal direction) p-refinement on boundary cells with Dirichlet boundary conditions. We use the method of manufactured solutions to derive forcing functions. All test problems use $\vec{b} = (1, 1)$ and $c = 2$.

4.3.1. The Necessity of Normal p-Refinement. An important part of the proof for Theorem 6 is the translation-invariant property of the discretization in the periodic direction. Numerical experiments, summarized in Figure 5, indicate that this is not merely a convenient assumption: in the case of interior bilinear elements, the discretization must be equivalent to a tensor product of two one-dimensional discretizations in order to obtain the improved convergence rates in the seminorms defined by Equations (2)-(3).

To demonstrate this, we consider discretizations with interior bilinear elements and either *normal p-refinement* or *isostropic p-refinement*, where the second case still uses continuity constraints to obtain a conforming solution. Notate the polynomial space on each boundary cell, $P^m \otimes P^{m+p}$, by $Q^{(m,m+p)}$, where m is the degree in the tangential direction and $m + p$ is the degree in the normal direction. These numerical experiments use the manufactured solution

$$
\begin{aligned}
u_1(x, y) =& (y^3 + \exp(-y^2) + \sin(4.5y^2) + \sin(20y)) \\
& \times (20\cos(4\pi x) + 0.1\sin(20\pi x) - 80\sin(6\pi x)).
\end{aligned}
$$
(139)

The results in Figure 5 show that the tensor-product structure of the discretization used in Theorem 6 is necessary for achieving improved boundary derivative convergence rates (i.e., order 2 for first derivatives and order 1 or 2 for second derivatives). Performing isotropic p-refinement (which results in a larger finite element space than p-refinement purely in the normal direction) does not improve the rates of convergence even though the approximation space is larger.

4.3.2. Extension to a Nonperiodic Boundary. Theorem 6 only applies to domains with periodic boundary conditions in one of the coordinate directions; however, numerical experiments indicate that the normal p-refinement scheme improves derivative convergence rates in more general geometries. To demonstrate this, we performed numerical experiments on a rectangular domain with Dirichlet boundary conditions, a $Q^{(1+p,1+p)}$ element in each corner (which corresponds to the tensor product of normal refinement in both directions), and $Q^{(1,1+p)}$ elements in the other boundary cells. Like the other 2D numerical experiments, we only consider bilinear elements ($Q^{(1,1)}$) on the interior of the domain. The manufactured solution in this test case, which is not periodic in either direction, is

(140) $u_2(x, y) = xy\sin(20y) + 10\exp(-xy)\cos(15x) + 2\sin(10^{y^2 + \cos(x)}) + \sin(30xy).$

Figure 6 summarizes the results of these experiments. These experiments show that the results proven in Theorem 6 generalize to a domain with purely Dirichlet boundary conditions.
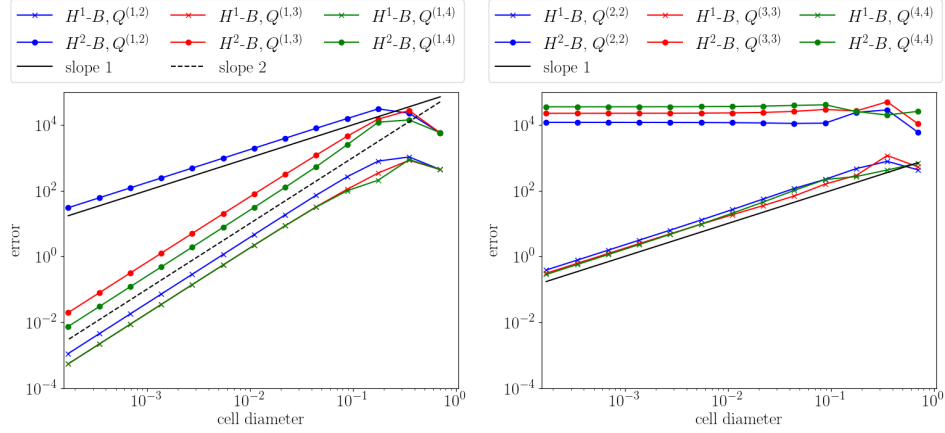
FIGURE 5. Rates of convergence for a solution to Equation (1) with periodic boundary conditions in the x direction. One set of discretizations uses p-refinement in just the normal direction (left, with the scheme proposed by Figure 1) and the other uses isotropic p-refinement (right). The boundary cell polynomial spaces are notated as $Q^{(m,m+p)}$. These results indicate that the tensor product structure assumed in Theorem 6 is necessary.
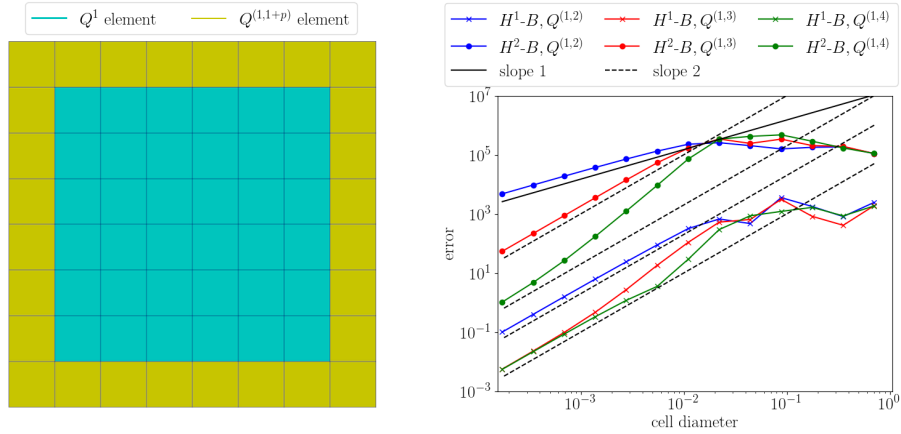

FIGURE 6. Depiction of the nonperiodic square domain and numerical convergence rates. The picture on the left shows which cells have been p-refined in the normal direction after three global grid refinements. The picture on the right shows the rates of convergence. This experiment shows that the asymptotic rates proven in Theorem 6 also hold when all boundaries are Dirichlet and the discretization has a tensor-product structure. It also shows (particularly in the H^2-B, $Q^{(1,4)}$ case) that the higher power of Δy (in that case 3) term in Theorem 6 dominates before the asymptotic rate (in that case 2) is reached.

4.3.3. Extension to a Disk With Radial p-Refinement. The final numerical example shows that the convergence rate proven in Theorem 6 holds in a non-Cartesian geometry. Consider a disk whose central cells are aligned with the x, y axes, cells near the boundary are aligned with the r, θ axes (i.e., they are rectangles in polar coordinates), and cells between these two regions are geometrically described with a transfinite interpolation between the Cartesian and polar regimes. This geometry description (i.e., Cartesian coordinates in the center, polar coordinates at the boundary, and a transfinite interpolation in between) results in a well-conditioned grid with boundary cells aligned with the polar coordinate axes after mesh refinement. A picture of the grid after one refinement is shown in Figure 7. Since the order of convergence under the seminorms defined by Equations (2)-(3) is second-order, we use the standard second-order bilinear mapping from the reference cell to the physical cell to perform all cell calculations. The manufactured solution in this test case is Equation (139).

Based on the results in Figure 7, we conjecture that the convergence rate proven in Theorem 6 holds for sufficiently regular grids where the cells near the boundary are aligned with the boundary itself (i.e., the cell faces are either orthogonal or parallel to the boundary). This implies that the proposed p-refinement strategy will improve boundary derivative convergence rates when the boundary of a domain is sufficiently smooth.

5. Concluding Remarks

This work proposed a new method for achieving higher-order accuracy in boundary derivative calculations while still using lower-order finite elements on the interior of the domain. The method, in essence, adds new degrees of freedom that enrich the boundary finite elements in a direction normal to the boundary itself. The numerical experiments imply that isotropic p-refinement does not improve the order of accuracy of boundary derivatives: put another way, the finite element space must have a tensor-product structure to obtain higher-order derivative convergence on the boundary. The proposed method resembles a finite difference discretization in the sense that the higher rate of convergence is available at all boundary vertices and that the rate of convergence in the first and second derivatives, after performing at least two levels of p-refinement, is equal to the global L^∞ rate of convergence.

There are several possible extensions of this work: one could derive a similar result to Theorem 6 by interpreting higher-order (e.g., biquadratic) basis functions as finite difference methods with nonuniform stencils. Another possible direction is finding a solid theoretical backing for the numerical examples given in Subsection (4.3.2) and Subsection (4.3.3), which show results for more general geometries than a square with periodic boundary conditions in the x direction. There are possibilities for extending the implementation as well: instead of Lagrange p-refinement, one could add degrees of freedom corresponding to normal derivatives on the boundary. Finally, since this method does not rely on any solution postprocessing procedures, it may be a useful technique to use in applications where one requires higher accuracy in the derivatives of a solution on a particular boundary and an energy estimate, such as complex boundary conditions for multiphysics applications.
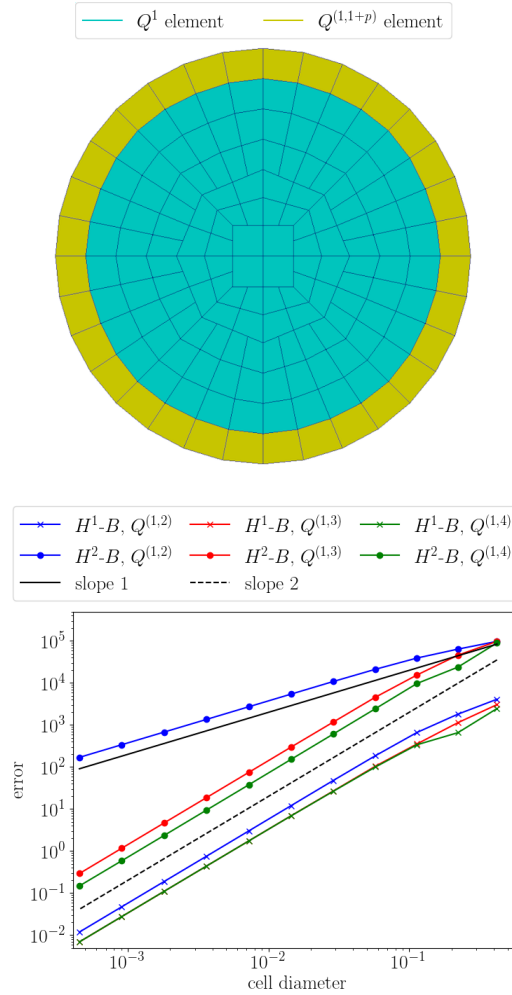
Acknowledgements

FIGURE 7. Depiction of the disk grid and numerical results. The picture on the left shows which cells have radial p-refinement after one global grid refinement and the picture on the right shows the rates of convergence: The H^1-B error plot for $Q^{(1,3)}$ is obscured by the plot for $Q^{(1,4)}$. These results show that the convergence rates proven in Theorem 6 apply to more general settings where the cells are aligned with a smooth boundary.

References

[1] M. Ainsworth and B. Senior. Aspects of an adaptive hp-finite element method: Adaptive strategy, conforming approximation and efficient solvers. *CMAME*, 150:65–87, 1997.

[2] D. Arndt, W. Bangerth, D. Davydov, T. Heister, L. Heltai, M. Kronbichler, M. Maier, J.-P. Pelteret, B. Turcksin, and D. Wells. The `deal.II` library, version 8.5. *Journal of Numerical Mathematics*, 2017.

[3] I. Babuška and T. Strouboulis. *The Finite Element Method and its Reliability*. Numerical Mathematics and Scientific Computation. Oxford Science Publications, 2001.

[4] I. Babuška and M. Suri. The optimal convergence rate of the p-version of the finite element method. *SIAM J. Numer. Anal.*, 24(4): 750-776, 1987.

[5] S. Balay, S. Abhyankar, M. F. Adams, J. Brown, P. Brune, K. Buschelman, L. Dalcin, V. Eijkhout, W. D. Gropp, D. Kaushik, M. G. Knepley, L. C. McInnes, K. Rupp, B. F. Smith, S. Zampini, and H. Zhang. PETSc users manual. Technical Report ANL-95/11 - Revision 3.7, Argonne National Laboratory, 2016.

[6] S. Balay, W. D. Gropp, L. C. McInnes, and Smith. B. F. Efficient management of parallelism in object oriented numerical software libraries. In E. Arge, A. M. Bruaset, and H. P. Langtangen, editors, *Modern Software Tools in Scientific Computing*, pages 163–202. Birkhäuser Press, 1997.

[7] W. Bangerth and H. Kayser-Herold. Data Structures and Requirements for hp Finite Element Software. *ACM Transactions on Mathematical Software*, 36, 2009.

[8] J. W. Banks and T. Hagstrom. On Galerkin Difference Methods. *J. Comp. Phys.*, 313:310–327, 2016.

[9] J. W. Banks, W. D. Henshaw, A. K. Kapila, and D. W. Schwendeman. An added-mass partition algorithm for fluid–structure interactions of compressible fluids and nonlinear solids. *J. Comp. Phys.*, 305:1037–1064, 2015.

[10] S. C. Brenner and L. R. Scott. *The Mathematical Theory of Finite Element Methods*, volume 15. Springer, 2002. Texts in Applied Mathematics.

[11] G. F. Carey. Derivative Calculation From Finite Element Solutions. *CMAME*, 35:1–14, 1982.

[12] G. F. Carey, S. S. Chow, and M. K. Seager. Approximate Boundary-Flux Calculations. *CMAME*, 50:107–120, 1985.

[13] P. G. Ciarlet. *The Finite Element Method for Elliptic Problems*, volume 40. Society of Industrial and Applied Mathematics, 2002. Classics in Applied Mathematics.

[14] J. Douglas Jr. and T. Dupont. Galerkin Approximations for the Two Point Boundary Problem Using Continuous, Piecewise Polynomial Spaces. *Numer. Math.*, 22:99–109, 1974.

[15] J. Douglas Jr., T. Dupont, and M. F. Wheeler. An L^∞ Estimate and a Superconvergence Result for a Galerkin Method for Elliptic Equations Based on Tensor Products of Piecewise Polynomials. *R.A.I.R.O.*, 8(2):61–66, 1974.

[16] J. Douglas Jr., T. Dupont, and M. F. Wheeler. A Galerkin Procedure For Approximating The Flux on the Boundary for Elliptic and Parabolic Boundary Value Problems. *R.A.I.R.O.*, 11(4):47–59, 1974.

[17] J. Douglas Jr., T. Dupont, and M. F. Wheeler. A Quasi-Projection Analysis of Galerkin Methods for Parabolic and Hyperbolic Equations. *Math. Comput.*, 32(142):345–362, Apr 1978.

[18] Evans, L. C. *Partial Differential Equations*, volume 19 of *Graduate Studies in Mathematics*. American Mathematical Society, 2007.

[19] H. Guo, Z. Zhang, and R. Zhao. Hessian Recovery For Finite Element Methods. *Math. Comp.*, 2016.

[20] R. Haberman. *Applied Partial Differential Equations*. Pearson, 2013.

[21] Lawrence Livermore National Laboratory. *hypre: High Performance Preconditioners.* `http://www.llnl.gov/CASC/hypre/`.

[22] P. Lax. *Functional Analysis*. Pure and applied mathematics. Wiley-Interscience, 2002.

[23] L. Li, W. D. Henshaw, J. W. Banks, D. W. Schwendeman, and A. Main. A stable partitioned FSI algorithm for incompressible flow and deforming beams. *J. Comp. Phys.*, 312:272–306, 2016.

[24] H. G. Roos, M. Stynes, and L. Tobiska. *Robust Numerical Methods for Singularly Perturbed Differential Equations: Convection-Diffusion-Reaction and Flow Problems.*, volume 24 of *Springer Series in Computational Mathematics*. Springer, second edition, 2008.

[25] Lars B. Wahlbin. *Superconvergence in Galerkin Finite Element Methods*. Lecture Notes in Mathematics. Spring, 1995.

[26] D. R. Wells. *Stabilized Reduced Order Models*. PhD thesis, Virginia Tech, 2015.

[27] M. F. Wheeler. An Optimal l_∞ Error Estimate for Galerkin Approximations to Solutions of Two-Point Boundary Value Problems. *SIAM J. Numer. Anal.*, 10(5):914–917, 1973.

[28] M. F. Wheeler. A Galerkin Procedure For Estimating The Flux For Two-Point Boundary Value Problems. *SIAM J. Numer. Anal.*, 11(4):764–768, Sep 1974.

[29] Z. Zhang and A. Naga. A New Finite Element Gradient Recovery Method: Superconvergence Property. *SIAM J. Sci. Comput.*, 26(4):1192–1213, 2005.

[30] O. C. Zienkiewicz and R. L. Taylor. *The Finite Element Method, Volume 1*. Butterworth Heinemann, 2000.

Appendices

A. Inequalities used to bound the Greens' function

(1)

(A.1)
$$\left|\frac{\exp(-z)-1}{z}\right| \le 1$$

as, if $\operatorname{Im}(z) = 0$, then the function is maximized as $z \to 0^+$, has negative slope for $z \ge 0$, and is bounded below by 0. If $\operatorname{Im}(z) \ne 0$ then by the maximum modulus principle this function is bounded above by the value of the analytic continuation along the boundary $\operatorname{Re}(z) = 0$, which is also 1. This implies that

(A.2)
$$\left|\frac{\exp(-2D\Delta x)-1}{2D}\right| \le \Delta x.$$

(2)

(A.3a)
$$\left|\frac{\exp(2DL)\pm\exp(2D\Delta x)}{\exp(2DL)-1}\right| \le 2\left|\frac{\exp(2DL)}{\exp(2DL)-1}\right|$$

(A.3b)
$$\le 2\frac{e}{e-1}$$

(A.3c)
$$\le 4$$

since $\operatorname{Re}(D)$ and L are greater than unity.

(3) If $L - \Delta x \le x \le L$ then

$$\left|\frac{\exp(-D(L+\Delta x-x))\pm\exp(D(L-\Delta x-x))}{2D}\right|$$

(A.4a)
$$\le \left|\frac{\exp(-D(L+\Delta x-x))}{2D}\right| + \left|\frac{\exp(D(L-\Delta x-x))}{2D}\right|$$

(A.4b)
$$\le \frac{1}{|D|}$$

since $0 \le L + \Delta x - x$ and $L - \Delta x - x \le 0$, so the arguments of both exponentials have negative real parts.

B. Bounding the ratio of exp and sinh

for $z = a + bI$ and $a > 0$:

(B.1a)
$$|\sinh(z)|^2 = (\cos(b)\cosh(a))^2 + (\sin(b)\sinh(a))^2$$

(B.1b)
$$\ge (\cos(b)\sinh(a))^2 + (\sin(b)\sinh(a))^2$$

(B.1c)
$$= (\sinh(a))^2$$

(B.1d)
$$\ge a^2$$

Hence, if $|b| \le |a|$

(B.2)
$$2|\sinh(z)| \ge |z|.$$

924

Hence

(B.3a)
$$\frac{\exp(z)}{\sinh(z)} = 2 + \frac{\exp(-z)}{\sinh(z)}$$

(B.3b)
$$\left| \frac{\exp(z)}{\sinh(z)} \right| = 2 + \left| \frac{\exp(-z)}{\sinh(z)} \right|$$

(B.3c)
$$\leq 2 + \frac{2}{|z|}$$

Department of Mathematics, University of North Carolina, Chapel Hill, NC USA
E-mail: `drwells@email.unc.edu,daverwells@gmail.com`

Department of Mathematical Sciences, Rensselaer Polytechnic Institute, Troy, NY USA
E-mail: `banksj3@rpi.edu`